Fermion Regge-Pole Model for the Structure of Pion-Nucleon Elastic Scattering in the Backward Hemisphere*

V. BARGER AND D. CLINE
Department of Physics, University of Wisconsin, Madison, Wisonsin
(Received 19 October 1966)

The $Y=+1$ fermion resonances that show up strongly in total-cross-section data are classified as Regge recurrences on three straight-line trajectories (namely, Δ_δ, N_γ, N_α) in a Chew-Frautschi plot. From extrapolations of the trajectories, resonance doublets are predicted in the vicinity of 2200 MeV (with $J^P=\frac{7}{2}^-$ and $\frac{9}{2}^+$) and 2630 MeV (with $J^P=11/2^-$ and $13/2^+$), due to recurrences of the N_γ and N_α trajectories at similar mass values. A model is constructed for π^-p elastic scattering near the backward direction based on interference of the direct-channel resonance amplitude (Δ_δ, N_γ, N_α) with the amplitude due to fermion Regge exchange (Δ_δ) in the crossed channel. The predictions of the model compare favorably with existing data on the energy dependence of the π^-p differential cross section at 180° center-of-mass scattering angle and the general shape of the π^-p angular distributions near 180°. The results confirm the consistency of the Regge-recurrence parity assignments with the scattering data. The resonance elasticities used in the calculations are roughly the same as the elasticities determined from total-cross-section data. The model is extended to π^+p elastic scattering at backward angles. In the π^+p process, the direct-channel Δ_δ resonance contribution alone saturates the experimental differential cross section in the backward cone at momenta below 4 BeV/c. Comparison with the π^+p backward-scattering data gives additional confirmation for the proposed Δ_δ Regge-recurrence parity assignments. In addition, the model supports the existence of an $I=\frac{3}{2}$ s-wave resonance at 1690 MeV. Finally, the polarization is predicted for $\pi^\pm p$ elastic scattering in the backward cone.

I. INTRODUCTION

A NUMBER of $Y=+1$ fermion resonance states of mass greater than 2 BeV have been reported from studies of $\pi^\pm p$ total-cross-section data.[1,2] Because of the large number of background partial waves that are present at such energies, it is unlikely that traditional phase-shift analyses will be useful in determining the spin-parity assignments of many of these high-mass resonances. Therefore, it is necessary to develop alternative techniques in order to determine the quantum numbers of these fermion resonance states.

Interference phenomena which arise from the interplay of a direct-channel fermion resonance amplitude with a known background amplitude provide a possible method for the study of resonances in the intermediate energy range. Successful application of the interference technique depends critically on a valid model for the background amplitude. If a dynamical theory exits for the background amplitude, then such a study can simultaneously provide a sensitive test of the dynamical model and also determine quantum numbers of the resonances. The interference effects in the differential cross section will be most dramatic in a process for which the background amplitude is of comparable size to the resonance amplitude. Nevertheless, in processes for which the direct and crossed amplitudes are not of comparable size, the polarization still provides a measure of the type of interference.

The interference technique was suggested by Heinz and Ross for backward π^+p elastic scattering using nucleon exchange in Born approximation as the background amplitude.[3] Recently, the technique has been successfully applied in detailed comparisons with the experimental data on (i) $\pi^-p\to p\pi^-$ scattering at 180° (using a Reggeized fermion-exchange background amplitude)[4] and (ii) $\pi^-p\to\pi^0n$ scattering amplitude at 0° (using a Reggeized rho-meson-exchange background amplitude).[5] From these two applications, appreciable information has already been obtained concerning dynamical exchange mechanisms and the properties of the $Y=+1$ fermion resonances.

The present paper is devoted to an extensive treatment of pion-nucleon elastic scattering in the backward hemisphere within the framework of the interference model. The underlying basis for all our calculations is the premise that the sum of the direct-channel resonance

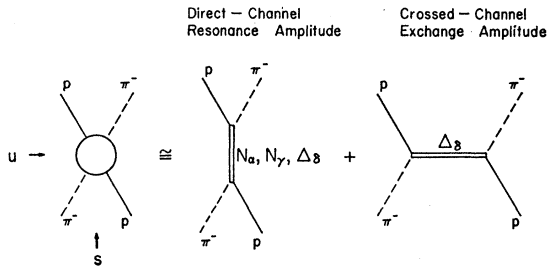

FIG. 1. Schematic illustration of the interference-model approximation for π^-p elastic scattering in the backward hemisphere. The scattering amplitude is represented as a sum of the direct-channel (Δ_δ,N_α,N_γ) resonance amplitude and the crossed-channel (Δ_δ) fermion-exchange amplitude.

* Work supported in part by the University of Wisconsin Research Committee, with funds granted by the Wisconsin Alumni Research Foundation, and in part by the U. S. Atomic Energy Commission under Contract AT(11-1)-881 No. COO-881-88.

[1] A. Citron *et al.*, Phys. Rev. **144**, 1101 (1966).

[2] A. H. Rosenfeld *et al.*, Rev. Mod. Phys. **37**, 633 (1965); Lawrence Radiation Laboratory Report No. 8030, August 1966 (unpublished); A. H. Rosenfeld, in Lectures at Yalta International School on Symmetry of Elementary Particles, 1966 (unpublished).

[3] R. Heinz and M. Ross, Phys. Rev. Letters **14**, 1091 (1965).

[4] V. Barger and D. Cline, Phys. Rev. Letters **16**, 913 (1966).

[5] V. Barger and M. Olsson, Phys. Rev. **151**, 1123 (1966).

amplitude and cross-channel exchange amplitude adequately represents the true physical scattering amplitude, as illustrated in Fig. 1 for $\pi^- p$ backward elastic scattering. The approximate consistency of resonance parameters determined from reactions with different background amplitudes (i.e., $\pi^- p \to \pi^0 n$ at 0° [5] and $\pi^- p \to p\pi^-$ at 180° [4]) suggests that this additive hypothesis for direct- and cross-channel amplitudes is a valid approximation.

In Sec. II, a Regge-recurrence classification scheme is proposed for the $Y=+1$ fermion resonances. An interference model for the phenomenological description of backward pion-nucleon elastic scattering is developed in Sec. III. In Sec. IV, the predictions of the model are compared with the existing experimental scattering data. Finally, a discussion of the validity of the theoretical model is presented in Sec. V. An extension of the Regge-recurrence classification scheme for $Y \neq 1$ fermion resonances is briefly discussed.

II. CHEW-FRAUTSCHI PLOT

In Reggeization of the pion-nucleon scattering amplitude, separate analytic continuations to complex J are required for partial-wave amplitudes of even- and odd-signature $\tau=(-)^{J-1/2}$ due to the existence of exchange forces. Thereby the physical resonance states associated with the trajectory of a given Regge pole are spaced by two units of total angular momentum J (but have the same parity P, isotopic spin I, etc.)[6]. *A priori*, the behavior of the trajectory $\alpha(\sqrt{u})$ as a function of energy $\sqrt{u}$ is unknown, other than the expectation that $\alpha(\sqrt{u})$ satisfy a dispersion relation[7]

$$\alpha(\sqrt{u})=\frac{1}{\pi}\int_{(M+\mu)}^{\infty}\frac{d\xi\,\mathrm{Im}\alpha(\xi)}{\xi-\sqrt{u}-i\epsilon}+\frac{1}{\pi}\int_{-(M+\mu)}^{-\infty}\frac{d\xi\,\mathrm{Im}\alpha(\xi)}{\xi-\sqrt{u}-i\epsilon},$$

with cuts starting at thresholds $\pm(M+\mu)$. Consequently, until the spins and parities of the observed resonances are experimentally determined, there exists no definite guideline to follow in the classification of the resonances as recurrences along Regge trajectories. Recurrences along a trajectory should occur for $\mathrm{Re}\alpha(M_R)=J_R$ and $\alpha'(M_R)>0$.

In order to construct a plausible empirical classification scheme of the observed baryon resonances according to the Regge-recurrence concept, we must at present rely heavily on the low-mass resonances for which the spin-parity (J^P) assignments are already experimentally established. Starting with the $I=\frac{3}{2}$ states, it is well known that the 1236- and 1924-MeV resonances are $\frac{3}{2}^+$ and $\frac{7}{2}^+$, respectively.[2] We accept these resonances as the first two members of a Δ_δ trajectory, and explore possible recurrence assignments for the $I=\frac{3}{2}$ resonances at 2450, 2840, and 3220 MeV.[1,5,8] The most economical scheme is to place these three higher-mass resonances on the Δ_δ trajectory, as indicated in the Chew-Frautschi plot[9] of Fig. 2(a). From the experimental masses of the resonances, the resulting form for $\mathrm{Re}\alpha(\sqrt{u})$ is found to be very well approximated by a straight line in the variable u.

Such an inductive procedure is also followed in assigning the negative parity $I=\frac{1}{2}$ resonances to the N_γ trajectory, as in Fig. 2(b). Here the 1512- and 2210-MeV resonances[8] are known to be $\frac{3}{2}^-$ and $\frac{7}{2}^-$, respectively.[2,10] A straight line with roughly the same slope as the Δ_δ trajectory passes smoothly through the 2210, 2640, and 3020 $I=\frac{1}{2}$ resonances,[1] but slightly deviates from the position of the 1512-MeV resonance.

The only known resonances remaining for a positive-parity $I=\frac{1}{2}$ trajectory N_α are the nucleon at 938 MeV with $J^P=\frac{1}{2}^+$ and the 1688-MeV resonance with $J^P=\frac{5}{2}^+$. A straight line through these two states extrapolates through $\frac{9}{2}^+$ at $\sim$2220 MeV and $(13/2)^+$ at $\sim$2610 MeV, as shown in Fig. 2(b). On the basis of the extrapolation, the resonance doublets $\{N_\gamma(2210, \frac{7}{2}^-); N_\alpha(2220, \frac{9}{2}^+)\}$ and $\{N_\gamma[2640, (11/2)^-]; N_\alpha[2610, (13/2)^+]\}$ are predicted to occur as recurrences of the N_γ, N_α trajectories at such similar mass values. The N_γ member of a resonance doublet has orbital momentum one unit lower than the N_α member. Thus, the N_γ member would be expected to have a larger elastic width than the N_α member of the doublet because of centrifugal-barrier factors[11] (provided that the radii of interaction and reduced widths are comparable). In such a circumstance, the contribution of the negative-parity N_γ resonance should dominate the contribution of the positive parity N_α. In total-cross-section data, the parity doublet would effectively show up as a single bump. The parity doublet in the vicinity of 2200 MeV can presumably be disentangled by a careful phase-shift analysis. Discovery of the missing N_α recurrences would provide a striking verification of the Regge-recurrence assignments based on the straight-line approximation to the real part of the trajectory function.

The classification of resonances as Regge recurrences in Fig 2 is at present necessarily limited to those states that show up strongly in total-cross-section data. Nonetheless, these same resonances are also expected to

[6] The notation for labeling trajectories is from A. H. Rosenfeld, in *Proceedings of the 1962 Annual International Conference on High-Energy Physics at CERN*, edited by J. Prentki (CERN, Geneva, 1962), p. 325. Symbols: $\Delta(Y=1, I=\frac{3}{2})$; $N(Y=1, I=\frac{1}{2})$. Subscripts: $\alpha(P=+, \tau=+)$; $\beta(P=-, \tau=+)$; $\delta(P=+, \tau=-)$; $\gamma(P=-, \tau=-)$.

[7] V. N. Gribov, Zh. Eksperim. i Teor. Fiz. **43**, 1529 (1962) [English transl.: Soviet Phys.—JETP **16**, 1080 (1963)].

[8] The quoted values for the masses of the Δ_δ resonances are based on the analysis of Ref. 5. The quoted values for the N_α and N_γ masses are best determinations from the present analysis or from Refs. 1, 2, or 5. Similar remarks apply to the resonance widths. It must be realized that the masses and widths of the resonances are not very precisely determined at present.

[9] G. F. Chew and S. C. Frautschi, Phys. Rev. Letters **7**, 394 (1961).

[10] A. Yokosawa *et al.*, Phys. Rev. Letters **16**, 714 (1966).

[11] See, for example, J. M. Blatt, and V. F. Weisskopf, *Theoretical Nuclear Physics* (John Wiley & Sons, Inc., New York, 1952), p. 361.

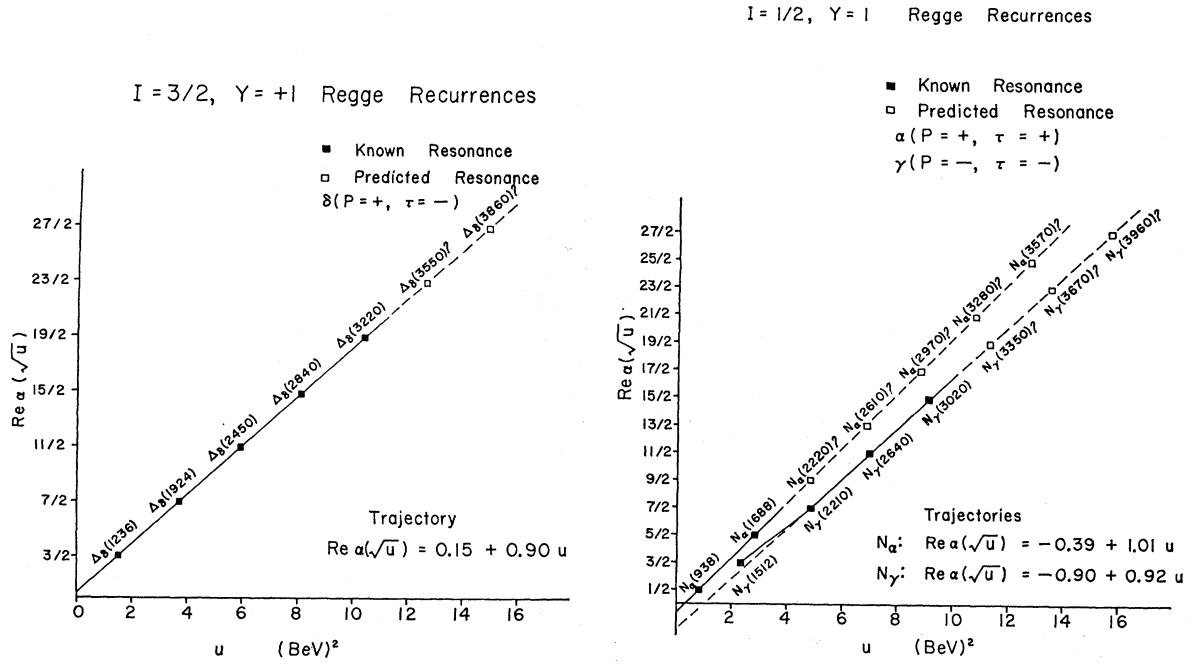

FIG. 2. Chew-Frautschi plot of the $Y=+1$ fermion Regge recurrences: (a) $I=\frac{3}{2}$ resonances; (b) $I=\frac{1}{2}$ resonances. Notation: parity P; signature $\tau=(-)^{J-1/2}$. All the resonances which show up strongly in total-cross-section data have been classified as recurrences.

play the dominant role in dynamical calculations. In this spirit, interference models based on the recurrences shown in Fig. 2 are constructed in Secs. III and IV for $\pi^{\pm}p$ elastic scattering near the backward direction.

III. STATEMENT OF INTERFERENCE MODEL

The pion-nucleon scattering amplitude can be expressed in a two-component form as

$$f(\sqrt{s},u)+i\boldsymbol{\sigma}\cdot\hat{n}\,\sin\theta g(\sqrt{s},u). \tag{1}$$

The variables $\sqrt{s}$ and θ are the center-of-mass energy and scattering angle; u is the square of the four-momentum transfer between pion and proton. The unit vector $\hat{n}$ is defined by $\hat{n}=(\mathbf{k}_f\times\mathbf{k}_i)/|\mathbf{k}_f\times\mathbf{k}_i|$, where $\mathbf{k}_f$ and $\mathbf{k}_i$ are the final- and initial-pion momenta, respectively. In terms of the amplitudes f and g, the differential cross section and polarization are given by

$$(d\sigma/d\Omega)(s,\theta)=|f|^2+\sin^2\theta|g|^2, \tag{2}$$

$$P_n(\theta)=\frac{2\sin\theta\,\mathrm{Im}(fg^*)}{|f|^2+\sin^2\theta|g|^2}. \tag{3}$$

Our subsequent calculations are based on the assumption that the pion-nucleon scattering amplitude near 180° is well represented by the *sum* of amplitudes[12] arising from (i) the direct s-channel contributions of the resonances on the Δ_δ, N_α, N_γ trajectories, and (ii) the crossed u-channel contributions from the Δ_δ, N_α, N_γ Regge poles (see Fig. 1). Thus, in Eqs. (1) and (2), we take

$$f=f^{\mathrm{Res}}+f^{\mathrm{Regge}},\qquad g=g^{\mathrm{Res}}+g^{\mathrm{Regge}}. \tag{4}$$

The explicit forms for the resonance amplitudes (f^{Res}, g^{Res}) and the Regge-exchange amplitudes (f^{Regge}, g^{Regge}) are discussed below.

A. Resonance Amplitude

The amplitude resulting from a Regge recurrence in the s-channel reduces to a Breit-Wigner resonance form for $\sqrt{s}$ in the vicinity of the mass of the physical resonance. We represent the total amplitude due to the successive recurrences as a sum of Breit-Wigner amplitudes for the known resonances. The contribution of a single direct-channel resonance of isotopic spin I to the isotopic-spin amplitudes f^I and g^I can be written as

$$f^I(\sqrt{s},u)=-\frac{1}{k}\frac{x_I(J+\frac{1}{2})}{\epsilon-i}P_l(\cos\theta),$$
$$g^I(\sqrt{s},u)=-\frac{1}{k}\frac{x_I(-)^{J-l+1/2}}{\epsilon-i}P_l'(\cos\theta), \tag{5}$$

where

$$P_l'(\cos\theta)=\frac{d}{d\cos\theta}P_l(\cos\theta),$$

with J and l as the total and orbital angular momenta

[12] A similar approximation for dynamical calculations in a strip model has been suggested by N. F. Bali, G. F. Chew, and S. Chu, Lawrence Radiation Laboratory Report No. UCRL-16961 (unpublished).

of the resonance, respectively. Here, k is the c.m. momentum and P_l is the Legendre function. In Eq. (5), x_I represents the elasticity parameter of the resonance and $\epsilon=(M_R^2-s)/M_R\Gamma$, where M_R and Γ are the mass and full width of the resonance.[13] Little is known regarding the proper momentum dependence of the elasticity or total width for a very inelastic resonance. Consequently, we make the simplest possible choice—constant x and Γ—as is done in the analyses of resonances from total-cross-section data.[1] This choice is dictated by the necessity of using resonance parameters determined from total-cross-section analyses. Thus, we implicity assume that the resonance form in Eq. (5) remains approximately valid away from the resonance position. The s-channel resonance contributions to the πN elastic and charge-exchange (c.e.) scattering amplitudes are obtained from Eq. (5) by the isotopic-spin relations

$$\begin{aligned} f^{\pi^-p}&=\tfrac{1}{3}(f^{3/2}+2f^{1/2}),\\ f^{\pi^-p}&=f^{3/2},\\ f^{\text{c.e.}}&=\tfrac{1}{3}\sqrt{2}(f^{3/2}-f^{1/2}), \end{aligned} \tag{6}$$

and the corresponding relations for the g amplitudes.

B. Fermion Regge-Exchange Amplitude

The amplitudes f and g of Eq. (1) can be expressed in terms of a single s-channel amplitude $f_1(\sqrt{s},u)$ as

$$\begin{aligned} f(\sqrt{s},u)&=f_1(\sqrt{s},u)-\cos\theta f_1(-\sqrt{s},u),\\ g(\sqrt{s},u)&=-f_1(-\sqrt{s},u). \end{aligned} \tag{7}$$

The crossing-symmetry relation which connects the s-channel amplitude $f_1(\sqrt{s},u)$ with the corresponding u-channel amplitude $f_1(\sqrt{u},s)$ is

$$f_1(\sqrt{s},u)=\frac{E_s+M}{2\sqrt{s}}\left[(\sqrt{u}-\sqrt{s}+2M)\frac{f_1(\sqrt{u},s)}{E_u+M}+(\sqrt{u}+\sqrt{s}-2M)\frac{f_1(-\sqrt{u},s)}{E_u-M}\right], \tag{8}$$

where $E_s=(s+M^2-\mu^2)/(2\sqrt{s})$ is the c.m. energy of the nucleon[14]; a corresponding definition holds for E_u.

The procedure of performing a Sommerfeld-Watson transformation on the u-channel partial-wave expansion of $f_1(\sqrt{u},s)$ and obtaining the contribution of a fermion Regge pole to πN elastic scattering has been discussed in detail by Singh.[15] The contribution of a fermion Regge pole with signature $\tau=(-)^{J-1/2}$ and parity $P=(-)^{l+1}$ to the amplitude $f_1(\sqrt{u},s)$ is given by

$$\begin{aligned} f_1(\sqrt{u},s)=&\frac{E_u+M}{\sqrt{u}}\frac{\beta(\pm\sqrt{u})}{\cos\pi\alpha(\pm\sqrt{u})}\left(\frac{q^2}{s_0}\right)^{\alpha(\pm\sqrt{u})-1/2}\\ &\times[\mathcal{P}'_{\alpha(\pm\sqrt{u})+1/2}(-z)+\tau\mathcal{P}'_{\alpha(\pm\sqrt{u})+1/2}(z)]\\ &-\frac{E_u-M}{\sqrt{u}}\frac{\beta(\mp\sqrt{u})}{\cos\pi\alpha(\mp\sqrt{u})}\left(\frac{q^2}{s_0}\right)^{\alpha(\mp\sqrt{u})-1/2}\\ &\times[\mathcal{P}'_{\alpha(\mp\sqrt{u})-1/2}(-z)-\tau\mathcal{P}'_{\alpha(\mp\sqrt{u})-1/2}(z)], \end{aligned} \tag{9}$$

where the upper signs in the arguments of α and β obtain for $\tau P=-1$ and the lower signs for $\tau P=+1$. The quantity $\beta(\sqrt{u})$ is essentially (up to a constant multiplicative factor) the residue of the Regge pole[15] at complex $J=\alpha(\sqrt{u})$. The trajectory $\alpha(\sqrt{u})$ is defined such that $\mathrm{Re}\alpha(\sqrt{u})$ will intersect the spin of a known resonance in Fig. 2 at positive $\sqrt{u}=M_R$. In Eq. (9), q and z are the u-channel c.m. momentum and cosine of the scattering angle, respectively.

$$\begin{aligned} q^2&=\{u-2M^2-2\mu^2+(M^2-\mu^2)^2/u\}/4,\\ z&=-\{s-M^2-\mu^2+u/2-(M^2-\mu^2)^2/2u\}/(2q^2). \end{aligned} \tag{10}$$

The functions $\mathcal{P}'_{\alpha\pm1/2}(z)$ are defined in terms of the Legendre function of the second kind as[16]

$$\mathcal{P}'_{\alpha\pm1/2}(z)=\frac{\cot\pi\alpha}{\pi}\mathcal{Q}'_{-(\alpha\pm1/2)-1}(z).$$

For scattered particles of equal mass (i.e., $M=\mu$), the u-channel scattering angle z would grow with s for fixed small u as

$$z\sim\left(-\frac{s-M^2-\mu^2}{2q^2}\right). \tag{11}$$

Then, for moderate values of s, the Legendre function would be well approximated by its leading term:

$$\mathcal{P}'_{\alpha+1/2}(z)\sim\frac{2\Gamma(\alpha+1)}{\Gamma(\frac{1}{2})\Gamma(\alpha+\frac{1}{2})}(2z)^{\alpha-1/2}. \tag{12}$$

We assume that the Regge-type behavior in Eqs. (11) and (12) also holds for unequal masses ($M\neq\mu$), despite the apparent kinematic limitation near $u=0$.[17] Rigorous justification for Regge behavior in the unequal-mass case of the form $s^{\alpha-1/2}$ has recently been presented.[18] In the interests of constructing a tractable phenomenological model, we shall retain only the leading term $(z)^{\alpha-1/2}$ from Eq. (9). Inserting Eqs. (11) and (12) into Eq. (9) yields the following result for the Regge-pole

[13] A number of different forms for the Breit-Wigner resonance amplitude have been suggested in the literature. For references, see S. R. Deans and W. G. Holladay, Vanderbilt University Report, 1966, (unpublished). We adopt the form discussed by W. Layson [Nuovo Cimento **27**, 724 (1963)] and J. D. Jackson [*ibid.* **34**, 1644 (1964)].

[14] Unless specified otherwise, M denotes the nucleon mass and μ the pion mass.

[15] V. Singh, Phys. Rev. **129**, 1889 (1963). Other sources on the theoretical treatment of fermion Regge poles can be found in Ref. 4.

[16] S. Mandelstam, Ann. Phys. (N. Y.) **19**, 254 (1962); M. Gell-Mann *et al.*, Phys. Rev. **133**, B159 (1964).

[17] D. A. Atkinson and V. Barger, Nuovo Cimento **38**, 634 (1965).

[18] D. Z. Freedman and J. Wang, Phys. Rev. Letters **17**, 569 (1966); M. L. Goldberger and C. E. Jones, *ibid.* **17**, 105 (1966).

contribution to the amplitude:

$$f_1(\sqrt{u},s)=\frac{E_u+M}{\sqrt{u}}\frac{2\Gamma(\alpha+1)}{\Gamma(\frac{1}{2})\Gamma(\alpha+\frac{1}{2})}\frac{1+ie\tau^{-i\pi\alpha}}{\cos\pi\alpha}\times\left(\frac{s-M^2-\mu^2}{s_0}\right)^{\alpha-1/2}. \quad (13)$$

The factor $\Gamma(\alpha+1)$ in Eq. (13) gives unphysical poles at $\alpha=-1, -2, \cdots$, which must be cancelled by zeros of the residue function β. The factor $1/\Gamma(\alpha+\frac{1}{2})$ produces zeros at $\alpha=-\frac{1}{2}, -\frac{3}{2}, \cdots$. Since our subsequent analysis involves only small negative α, we retain only the zeros at $\alpha=-\frac{1}{2}$ and $\alpha=-\frac{3}{2}$. Introducing an effective residue function,

$$\gamma(\pm\sqrt{u})=\beta(\pm\sqrt{u})\frac{2\Gamma(\alpha(\pm\sqrt{u})+1)}{\Gamma(\frac{1}{2})\Gamma(\alpha(\pm\sqrt{u})+\frac{5}{2})}, \quad (14)$$

the final form of the Regge-pole amplitude becomes

$$f_1(\sqrt{u},s)=\frac{E_u+M}{\sqrt{u}}(\alpha+\tfrac{1}{2})(\alpha+\tfrac{3}{2})\gamma\frac{1+i\tau e^{i\pi\alpha}}{\cos\pi\alpha}\times\left(\frac{s-M^2-\mu^2}{s_0}\right)^{\alpha-1/2}, \quad (15)$$

where the functional dependence of α and γ is on $(+\sqrt{u})$ for $\tau P=-1$ and on $(-\sqrt{u})$ for $\tau P=+1$, as in Eq. (9). Note that $f_1(\sqrt{u},s)$ in Eq. (15) goes through zero as $\alpha\to-\frac{1}{2}$ for $\tau=+$ or as $\alpha\to-\frac{3}{2}$ for $\tau=-$.[19] We now make some simplifying assumptions regarding the behavior of the trajectory and residue functions.

The Chew-Frautschi plot in Sec. II suggests that trajectories of the form

$$\mathrm{Re}\alpha(\sqrt{u})=a+bu \quad (16)$$

adequately interpolate through the masses of the known resonances. For the purposes of estimating $\alpha(\sqrt{u})$ in Eq. (15), we make the simplest possible assumption that this form for $\alpha(\sqrt{u})$ remains approximately valid in the scattering region under consideration. [Note that this assumes $\alpha(\sqrt{u})$ to be real for $u<(M+\mu)^2$.][20,21]

We also assume that the effective residues $\gamma(\sqrt{u})$ have no zeros for these values of u. The scaling factor s_0 in Eq. (15) is chosen for each Regge pole in the spirit of reducing the functional dependence of the corresponding residue $\gamma(\sqrt{u})$ on $\sqrt{u}$. In the actual data analysis in Sec. IV, we treat the effective residues as constant. However, this approximation is only expected to be valid for the limited range of u values near $u=0$.[22] With these approximations (namely, constant γ and $\alpha=a+bu$), we obtain from Eqs. (7), (8), and (15) the contribution of a fermion Regge pole to the f and g amplitudes

$$f=(1/\sqrt{s})[(E_s+M)-\cos\theta(E_s-M)]R(u,s), \quad (17)$$
$$g=-(1/\sqrt{s})(E_s-M)R(u,s),$$

where

$$R(u,s)=(\alpha+\tfrac{1}{2})(\alpha+\tfrac{3}{2})\gamma\frac{1+i\tau e^{-i\pi\alpha}}{\cos\pi\alpha}\left(\frac{s-M^2-\mu^2}{s_0}\right)^{\alpha-1/2}.$$

The isotopic spin relations

$$f^{\pi^-p}=f^{\Delta}$$
$$f^{\pi^+p}=\tfrac{1}{3}(f^{\Delta}+2f^{N}) \quad (18)$$
$$f^{\mathrm{c.e.}}=\tfrac{1}{3}\sqrt{2}(f^{\Delta}-f^{N})$$

are to be used in adding up the $\Delta(I=\frac{3}{2})$ and $N(I=\frac{1}{2})$ fermion Regge-exchange contributions to the f and g amplitudes for πN elastic and charge-exchange scattering.

IV. COMPARISON WITH EXPERIMENT

A. π^-p Elastic Scattering at 180°

The basic motivation for the interference model originated with a recent experiment at the zero-gradient syncrotron in which the differential cross section for π^-p elastic scattering was measured at a fixed angle of 180° over the laboratory momentum range 1.6–5.3 BeV/c.[23] The 180° differential cross section showed considerable structure as a function of laboratory momentum. The theoretical model of Secs. II and III provides a natural explanation of this structure as the interference of direct-channel Regge recurrences

[19] C. Chiu and J. Stack (private communication) have considered the consequences of the zero at $\alpha=-\frac{1}{2}$ for the N_α-exchange amplitude in π^+p scattering at high energy.

[20] This form is only meant as a crude approximation to $\alpha(\sqrt{u})$, adequate to fit present data. The actual power series expansion of $\alpha(\sqrt{u})$ around $u=0$ has, in general, odd terms in $\sqrt{u}$, and does not converge beyond the branch points at $\sqrt{u}=\pm(M+\mu)$. If odd terms in $\sqrt{u}$ were also present, then $\alpha(\sqrt{u})$ would also have an imaginary part for $u<0$.

[21] From the McDowell symmetry relation, a Regge pole at $J=\alpha(\sqrt{u})$ with residue $\beta(\sqrt{u})$ and quantum numbers τ, P must be accompanied by a Regge pole at $J=\alpha(-\sqrt{u})$ with residue $-\beta(-\sqrt{u})$ and quantum numbers τ, $-P$ (Ref. 15). Formally, trajectories of the form in Eq. (16) seem to imply the existence of additional resonance states (with the same J but opposite parity) at the positions of the known resonances. However, such speculation depends on the detailed behavior of the residue function at large values of $\pm\sqrt{u}$, which is beyond the scope of the present analysis of the scattering data near $u=0$. The possible existence of such resonance states has been discussed by I. A. Sakmar [Phys. Rev. **135**, B249 (1964)], C. Chiu and J. Stack (private communication), and B. Desai [Phys. Rev. Letters **17**, 498 (1966)].

[22] In particular, the magnitude of $\gamma(0)$ is not necessarily expected to be the same as $\gamma(M_R)$. For the Δ_δ Regge pole, the relation between $\gamma(M_R)$ and the width of the (3,3) resonance is

$$\gamma(M_R)=\frac{\pi\epsilon_R s_0}{16}\frac{M_R}{E_R+M}\frac{\Gamma}{q_R{}^3},$$

where

$$\epsilon_R=\left.\frac{d\alpha(\sqrt{u})}{d\sqrt{u}}\right|_{\sqrt{u}=M_R}.$$

For the N_α Regge pole, the corresponding relation is $\gamma(M_N)=-3\epsilon_N g^2/32$, where $g^2/4\pi\simeq15$.

[23] S. W. Kormanyos, A. D. Krisch, J. R. O'Fallon, K. Ruddick, and L. G. Ratner, Phys. Rev. Letters **16**, 709 (1966).

TABLE I. Experimental parameters for $Y=+1$ fermion resonance states. The predicted values of spin-parity J^P for the Regge recurrences are based on straight-line extrapolations in a Chew-Frautschi plot. The elasticity parameters x_I are based on the proposed J assignments. The unclassified states are the resonance candidates reported in recent phase-shift analyses (Ref. 24).

Resonance[a] (mass in MeV)	Spin-parity[b] (J^P)	Width[a] (BeV)	Elasticity (x_I) determinations: $\pi^-p\to p\pi^-$ at 180°	$\pi^-p\to\pi^0n$[d] at 0°	Total cross sections[e]	Phase shifts[f]
		Regge recurrences				
$\Delta_\delta(1236)$	$(3/2)^+$ est.	0.12	1.0	1.0	1.0	1.0
$\Delta_\delta(1924)$	$(7/2)^+$ est.	0.17	0.35–0.50[g]	0.49	0.33–0.41	0.50
$\Delta_\delta(2450)$	$(11/2)^+$	0.28	0.12	0.12	0.11	···
$\Delta_\delta(2840)$	$(15/2)^+$	0.40	0.05	0.03	0.03	···
$\Delta_\delta(3220)$	$(19/2)^+$	0.44	0.02	0.003	0.006	···
$N_\gamma(1512)$	$(3/2)^-$ est.	0.12	0.60	0.77	0.76	0.50–0.71
$N_\gamma(2210)$	$(7/2)^-$ est.	0.24	0.20	0.25	0.15–0.25	···
$N_\gamma(2640)$	$(11/2)^-$	0.40	0.05	0.08	0.07	···
$N_\gamma(3020)$	$(15/2)^-$	0.40	0.015	0.011	0.007	···
$N_\gamma(3350)$?	$(19/2)^-$	0.10	0.003–0.01	0.003	···	···
$N_\alpha(938)$	$(1/2)^+$ est.	···	···	···	···	···
$N_\alpha(1688)$	$(5/2)^+$ est.	0.10	0.60	1.04	0.80	0.66
$N_\alpha(2220)$?	$(9/2)^+$	0.20	0.05	···	···	···
$N_\alpha(2610)$?	$(13/2)^+$	0.30	0.025	···	···	···
$N_\alpha(2970)$?	$(17/2)^+$	···	···	···	···	···
		Unclassified states				
$N_\alpha(\sim1470)$	$(1/2)^+(P_{11})$	0.2	···	···	···	0.60–0.70
$N_\beta(\sim1560)$	$(1/2)^-(S_{11})$	0.28	···	···	···	0.40
$N_\beta(\sim1650)$	$(5/2)^-(D_{15})$	0.13	0.20	···	···	0.20–0.40
$\Delta_\beta(\sim1690)$	$(1/2)^-(S_{31})$	0.15–0.23	0.30	···	···	0.25–0.44
$N_\beta(\sim1715)$?	$(1/2)^-(S_{11})$	···	···	···	···	0.90

[a] References 1, 2, and 8.
[b] "Est." means "established."
[c] Present analysis. Also, see Ref. 4.
[d] Reference 5.
[e] References 1, 2. Additional sources given in Ref. 4.
[f] Reference 24.
[g] Elasticity of 0.35 used in π^-p analysis; elasticity of 0.50 used in π^+p analysis.

with a fermion-exchange background.[4] Since the u channel is in a pure $I=\frac{3}{2}$ state for the π^-p reaction, the Δ_δ is the only known trajectory in Fig. 2 that contributes to the exchange amplitude. In the straight-line approximation to the Δ_δ trajectory, a least-squares fit to the masses of the Δ_δ resonances in the Chew-Frautschi plot of Fig. 2(a) gives

$$\mathrm{Re}\alpha(\sqrt{u})=0.15+0.9u. \tag{19}$$

We use this form for $\alpha(\sqrt{u})$ in calculating the Δ_δ exchange amplitude from Eq. (17). The Δ_δ residue function γ is taken to be constant and of the same sign as the residue at the position of the (3,3) resonance.[22] The scaling factor s_0 is fixed at $s_0=0.4$ (BeV)^2 for the analysis. In the constant-residue approximation, this choice of s_0 is dictated by the slope

$$\left(\frac{d}{du}\ln\frac{d\sigma}{d\Omega}\right)_{u\cong0}$$

at the highest momentum for which data are available (8 BeV/c); here, the direct-channel contributions are expected to be small.

The direct-channel amplitude for π^-p scattering receives contributions from the resonances on the $(\Delta_\delta,N_\alpha,N_\gamma)$ trajectories. At 180°, the amplitude due to the successive recurrences [see Eqs. (5) and (6)] reduces to

$$f^{\mathrm{Res}}(180°)=\frac{1}{k}\left[\tfrac{1}{3}\sum_{\Delta_\delta}\frac{(-)^l(J+\frac{1}{2})x_{3/2}}{\epsilon-i}+\tfrac{2}{3}\sum_{N_\alpha,N_\gamma}\frac{(-)^l(J+\frac{1}{2})x_{1/2}}{\epsilon-i}\right], \tag{20}$$

where $\epsilon=(M_R{}^2-s)/(M_R\Gamma)$. The sums in Eq. (20) refer to the $(\Delta_\delta,N_\alpha,N_\gamma)$ resonance states listed in Table I. The factor of $(-)^l$ in Eq. (20) determines whether a particular resonance interferes constructively or destructively with the Δ_δ-exchange amplitude of Eq. (17). Thus, the observed interference pattern in the energy dependence of the 180° differential cross section provides a sensitive test of the proposed *parity assignments* of the resonances based on the Regge-recurrence classification scheme of Fig. 2. The resonance parameters (Γ,M_R) used in Eq. (20) are taken from Table I.[8] For starting values of the elasticity parameters (x_I), we used representative results from previous determinations,[1,2,5,10,24,25] as listed in the final three columns of Table I. Only the product $(J+\frac{1}{2})x_I$ is determined by

[24] C. Lovelace, in Proceedings of the Thirteenth International Conference on High-Energy Physics, Berkeley, 1966 (unpublished); P. Bareyre *et al.*, Phys. Letters **18**, 342 (1965); A. Donnachie *et al.*, *ibid.* **19**, 146 (1965); B. H. Bransden *et al.*, *ibid.* **19**, 420 (1966); R. J. Cence, *ibid.* **20**, 306 (1966); L. D. Roper *et al.*, Phys. Rev. **138**, B190 (1965).
[25] Sources of elasticity determinations from total-cross-section data are given in Ref. 4.

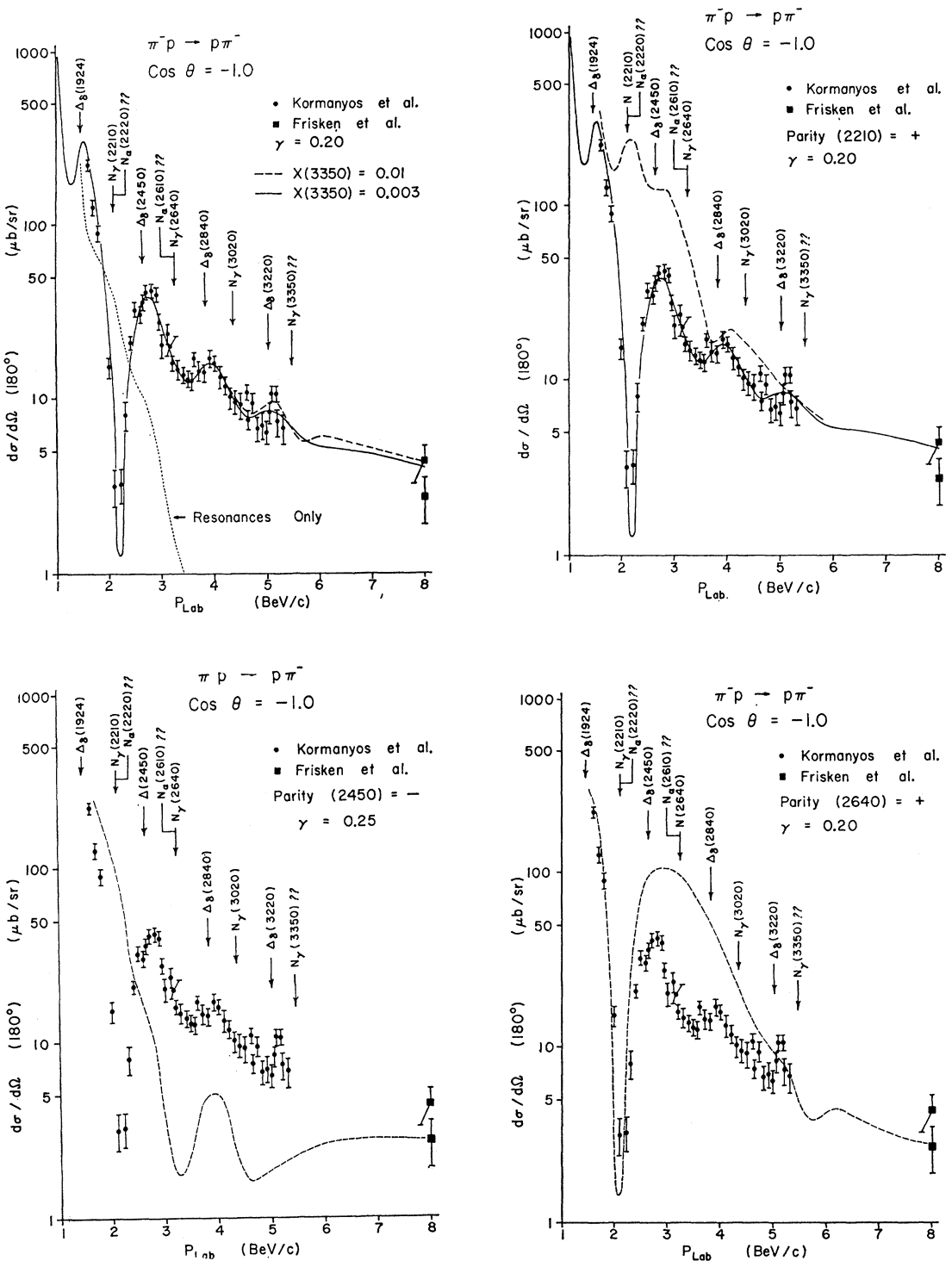

FIG. 3. (a) Theoretical curve for the 180° $\pi^- p$ elastic-scattering differential cross section as a function of laboratory momentum. The arrows indicate the positions of the direct-channel Δ_δ, N_α, and N_γ recurrences. The dotted curve represents the contributions of the resonances alone (no Δ_δ-exchange contribution). The dashed curve indicates the effect of increasing the elasticity of the $N_\gamma(3350)$ resonance. Experimental data are taken from Refs. 23 and 27. Normalization errors of $\pm 12\%$ are not shown. (b) The dashed curve is the theoretical result obtained with a positive-parity assignment for $N(2210)$, using the same parameters as for the solid curve of Fig. 3(a). (c) The dashed curve is the theoretical result obtained with a $P=-$assignment for $\Delta(2450)$. (d) The dashed curve is the theoretical result obtained with a $P=+$assignment for $N(2640)$.

most analyses. Values of the elasticity parameters in Table I are based on the Regge-recurrence J assignments. The elasticity determinations from $\pi^-p \to \pi^0 n$ at 0° were determined from a simultaneous analysis of $[\sigma_t(\pi^-p)-\sigma_t(\pi^-p)]$ and the forward charge-exchange differential cross section using a Regge ρ-meson exchange amplitude.[5] The elasticities obtained from total cross sections were determined without the use of a theoretical model by assuming smooth background amplitudes.[1,2,25] The phase-shift analyses[10,24] exist only for resonances of mass below 2.2 BeV. Only a phase-shift analysis can disentangle two resonances with different quantum numbers at the same mass position. For such cases of two resonances with the same mass, only a mean resonance height is determined from either the $\pi^-p \to \pi^0 n$ anslysis at 0° or the total-cross-section analysis. [For example, the fact that the effective elasticity parameter of $N_\alpha(1688)$ is greater than 1.0 from the $\pi^-p \to \pi^0 n$ analysis at 0° (see Table I)[5] presumably reflects the presence of resonating D_{15}, S_{31}, and S_{11} partial waves in the vicinity of 1688 MeV.[24]] A similar complication will arise at the positions of the predicted resonance doublets $\{N_\gamma(2210), \frac{7}{2}^-), N_\alpha(2220, \frac{9}{2}^+)\}$ and $\{N_\gamma[2640, (11/2)^-], N_\alpha[2610, (13/2)^+]\}$.

In addition to the resonances that can be assigned to the $(\Delta_\delta, N_\alpha, N_\gamma)$ trajectories, other resonances suggested by recent phase-shift analyses[2,24] are listed in Table I as unclassified states. The exact values of resonant energies and widths of these states are not known; in fact, some phase-shift solutions do not exhibit all of these resonances. For the most part, the direct-channel contributions of these unclassified resonances are dominated by the contributions of the $(\Delta_\delta, N_\alpha, N_\gamma)$ recurrences. Of these unclassified resonances, we include only the $N_\beta(\sim 1650)$ in Eq. (20). Arguments based on expected trajectory intercepts at $u \approx 0$ on a Chew-Frautschi plot also indicate that these unclassified states should not contribute appreciably to the exchange amplitude of Eq. (17).

As a first approach in investigating the validity of the interference model,[4] we calculated the 180° π^-p differential cross section using $\alpha(\sqrt{u})$ from Eq. (19) and the previously reported resonance parameters (M_R, Γ, x_I) for the *known* resonances on the $(\Delta_\delta, N_\alpha, N_\gamma)$ trajectories. The residue γ was essentially the only free parameter in this calculation. The high-energy data severely restricts the choice of γ. No appreciable variation of the x_I from their experimental values was allowed. This calculation produced reasonable qualitative agreement with the data, particularly in light of uncertainties in the elasticity parameters, masses, and widths of the resonances. Next, the predicted resonances $N_\alpha(2220, \frac{9}{2}^+)$, $N_\alpha[2610, (13/2)^+]$ were also included in the direct-channel amplitude. In addition, we have included $N_\gamma(3350)$, for which there is some evidence from total cross sections [5,26] The elasticity parameters of all the resonances were then slightly adjusted to yield quantitative agreement with the π^-p 180° differential-cross-section data. The final values for the elasticities are given in Table I. The theoretical π^-p differential cross section for $\gamma = 0.20$ BeV^{-1} is shown in Fig. 3(a) along with the 180° experimental data.[23,27] The calculation is in apparent good agreement with experiment over the entire momentum range, 1.6–8.0 BeV/c. It should be emphasized that the theoretical curve in Fig. 3(a) represents the absolute differential cross section and does not involve an arbitrary normalization. The resonance contribution alone to the differential cross section is shown by the dotted curve in Fig. 3(a). It is apparent that the amplitude due to the direct-channel resonances cannot, by itself, accommodate the principle features of the experimental data.

In order to test the Regge-recurrence parity assignments, the calculation has been repeated with opposite parity assignments to that given in Table I for *individual* ones of the higher mass resonances. Typical results are shown in Fig. 3(b), where $P=-$ for $N(2210)$,[28] in Fig. 3(c), where $P=-$ for $\Delta(2450)$, and in Fig. 3(d) where $P=+$ for $N(2640)$. It is apparent that changes in the parities yield qualitative disagreement with the experimental trend of $d\sigma/d\Omega$. Thus, we conclude that there is strong evidence for the parity assignments given in Table I according to the Regge-recurrence hypothesis.

In order to elucidate the interference between f^{Regge} and f^{Res}, the real and imaginary parts of the amplitudes are presented in Fig. 4 as a function of laboratory momentum. The two-decade valley in $d\sigma/d\Omega$ near $p_{\text{lab}} = 2.1$ BeV/c results from almost complete cancellation of f^{Regge} and f^{Res}, as shown in Fig. 4(a). In view of the fact that the relative size (and also sign) of the real and imaginary parts of f^{Regge} is tied to its energy dependence through $\alpha(\sqrt{u})$ [see Eq. (17)], it is rather remarkable that this amplitude allows just the proper interference to yield the results in Fig. 3(a). In addition, f^{Regge} has roughly the proper magnitude to explain the 8-BeV point where resonance contributions are negligible [see Fig. 4(a)]. In Figs. 4(b) and Fig. 4(c), the real and imaginary amplitudes at 180° are shown for low laboratory momenta. It is clear that the direct-channel amplitude dominates the exchange amplitube in the low-momentum region. This is fortunate, inasmuch as we have no basis for the approximate form of the Regge amplitude at very low momenta.

To summarize, the proposed model represents an internally consistent picture for both the $Y=+1$ fermion Regge recurrences and the experimental data on the 180° π^-p differential cross section. In the next section, the predictions of the model are compared with

[26] G. Hohler *et al.*, Phys. Letters **21**, 223 (1966).

[27] W. R. Frisken *et al.*, Phys. Rev. Letters **15**, 313 (1965); also revised data, 1966 (unpublished).

[28] The phase-shift analysis in Ref. 10 confirmed that the dominant resonating $I=\frac{1}{2}$ state in this vicinity was $\frac{7}{2}^-$. A similar conclusion was inferred in Ref. 23.

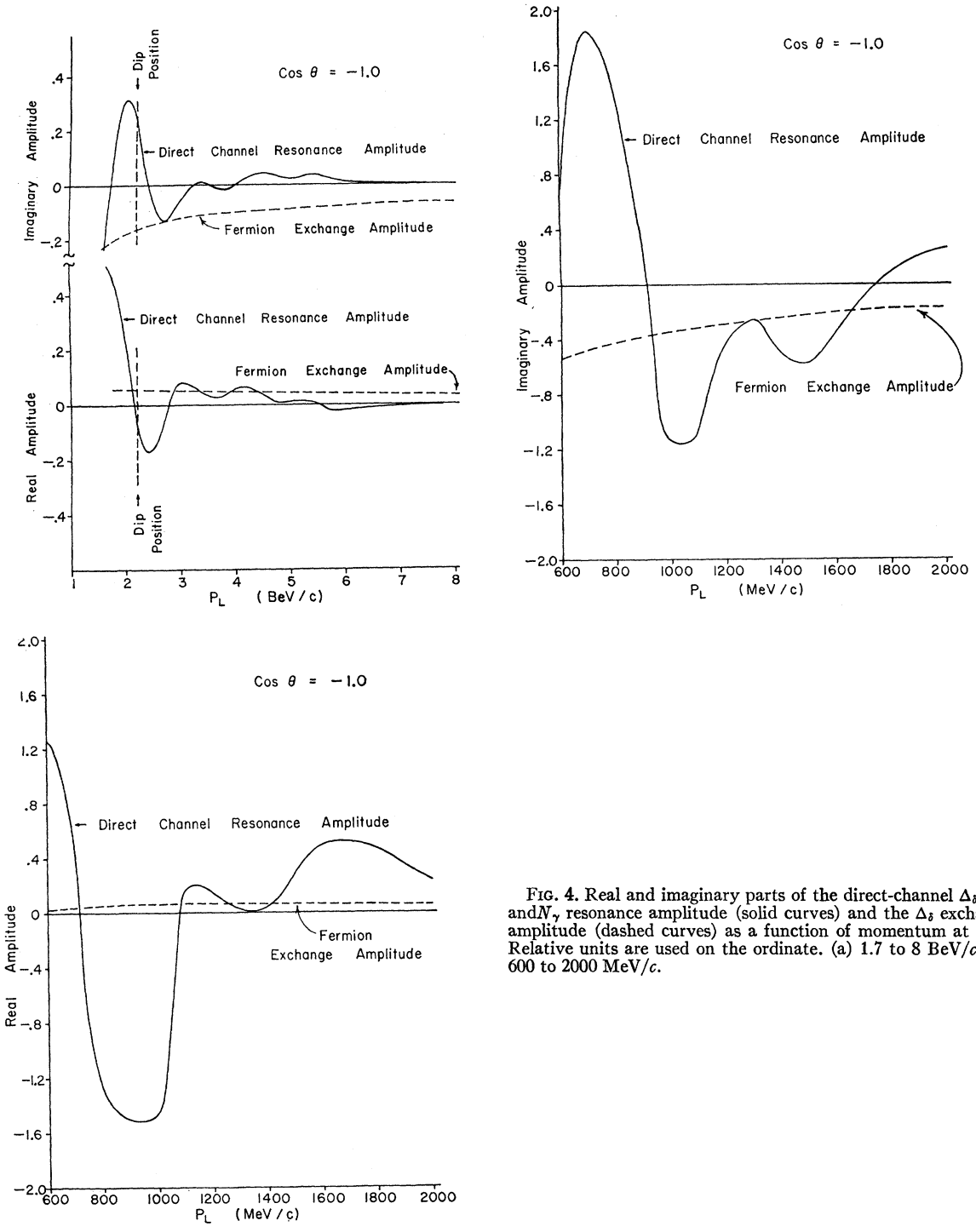

FIG. 4. Real and imaginary parts of the direct-channel Δ_δ, N_α, and N_γ resonance amplitude (solid curves) and the Δ_δ exchange, amplitude (dashed curves) as a function of momentum at 180°. Relative units are used on the ordinate. (a) 1.7 to 8 BeV/c; (b) 600 to 2000 MeV/c.

the experimental $\pi^- p$ angular distributions in the backward hemisphere.

B. $\pi^- p$ Angular Distributions Near 180°

In the preceding analysis of the 180° scattering, the Δ_δ Regge-exchange amplitude of Eq. (17) was specified by the following parameters:

$$\begin{aligned} &\text{residue}=\gamma=0.20\ \text{BeV}^{-1},\\ &\text{scaling factor}=s_0=0.4\ (\text{BeV})^2,\\ &\text{trajectory}=\alpha(\sqrt{u})=0.15+0.9u. \end{aligned} \tag{21}$$

In the constant-residue approximation employed here,

these parameters also determine the Regge amplitude of Eq. (17) for *near-backward* scattering. Similarly, the direct-channel resonance amplitude of Eq. (5) is completely specified for near-backward scattering by the elasticities x_I of the 180° analysis and the Regge recurrence (J,l) assignments. Therefore, within the framework of this model, the $\pi^- p$ angular distributions near 180° can now be predicted with no arbitrary parameters involved.

A limited amount of experimental data on $\pi^- p$ angular distributions exists at ten different laboratory momenta ranging from 1.7 to 8.0 BeV/c.[23,27,29] This data is shown in Fig. 5, along with the predictions of the model (solid curves). The contribution of the Δ_δ Regge-exchange amplitude alone (no resonance amplitude) is indicated by the dashed curves in Fig. 5. This exchange amplitude provides the dominant contribution to $d\sigma/d\Omega$ at 8.0 BeV/c; the angular distribution at this momentum was used in the selection of s_0 as given in Eq. (21). The experimental angular distributions in Fig. 5 exhibit either a sharp turn over or a rapid fall-off near 180°. This characteristic behavior alternates as a function of momentum. The model fairly well reproduces this effect as a result of interference between the resonances and the Regge background. The predicted angular distributions are not in detailed quantitative agreement at every momentum. In particular, there seems to be an appreciable deviation from the experimental points at 2.5 BeV/c. However, it should be noted that the theoretical curves were not fitted to the data. Moreover, the present data have large errors. As might be expected, the agreement with the data becomes less favorable away from backward angles. A number of complications which might arise in the extension of the model away from the backward direction are: (i) Tails of meson-exchange amplitudes from the t channel may become more important at smaller angles; (ii) resonances in lower partial waves could make relatively larger contributions at certain angles (since the contributions of the dominant resonances have minima, due to the structure in Legendre polynomials of large l); (iii) the linear form for the Regge trajectory α may break down at negative values of u. Nevertheless, within the framework of this admittedly crude model, the agreement with the experimental data seems to be reasonable.

In the analysis of $\pi^- p \to \pi^0 n$ at 0° in terms of Regge ρ-meson-exchange and direct-channel resonances, the theoretical model turned out to be approximately valid[5] down to 700 MeV/c. A similar feature seems to hold true in the backward $\pi^- p \to p\pi^-$ analysis. In Fig. 6, the theoretical model is compared with the available data in the momentum range 600–1900 MeV/c.[23,30] In this momentum range, the resonances provide the dominant contributions to $d\sigma/d\Omega$ [see Figs. 4(b), 4(c)]. Nevertheless, the over-all consistency of the model with experiment indicates that the Regge form of Eq. (17) does not produce disagreement with the data at very low momenta.

C. $\pi^- p$ Polarization Near 180°

The polarization of the recoil nucleon can be readily predicted as a function of momentum and angle from Eqs. (3), (5), and (17), using the Regge parameters of Eq. (21) and the resonance parameters of Table I. In the model, the Regge-exchange amplitude of Eq. (17) is a function of $(\sqrt{u})^2$ near the backward direction, and, hence, no contributions to the polarization arise from interference of the $\alpha(\sqrt{u})$ trajectory with the McDowell-reflected $\alpha(-\sqrt{u})$ trajectory.[31] Therefore, this Regge-exchange amplitude, by itself, leads to zero polarization. The predicted polarization is shown by the solid curve in Fig. 7(a) as a function of laboratory momentum at a fixed angle of $\cos\theta = -0.96$. The polarization oscillates in the momentum range 2 to 5 BeV/c and becomes relatively large, negative, and nonoscillatory at higher momenta. Since the resonance tails become dominantly real away from the resonance positions [see Eq. (5) or Fig. 4], the contribution of the resonances alone to the polarization is relatively small above 5 BeV/c, as indicated by the dashed curve of Fig. 7(a). Thus, at high momenta, the polarization comes almost entirely from the cross product of the Regge and resonance amplitudes. This characteristic is a distinguishing feature of this type of model. Finally, for comparison, the dash-dot curve of Fig. 7(a) indicates the amount of polarization which results when the high-mass resonances $\Delta_\delta(2850)$, $\Delta_\delta(3220)$, $N_\gamma(3020)$, and $N_\gamma(3350)$ are omitted from the direct-channel amplitude. This curve illustrates that, in this model, the tails of the lower-mass resonances still play an important role in polarization at high laboratory momenta. However, this prediction may be somewhat modified if energy-dependent resonance widths turn out to be necessary. The changes in the angular dependence of the predicted polarization as a function of laboratory momentum are shown in Fig. 7(b). At all momenta, the polarization rises to a maximum at $\cos\theta \sim -0.98$. The predicted variation of the polarization with energy and angle provides a sensitive method for study of the detailed formulation of the interference model.

[29] W. Busza, D. G. Davis, B. G. Duff, F. F. Heymann, C. C. Nimmon, D. T. Walton, E. H. Bellamy, T. F. Buckley, P. V. March, A. Stefanini, and J. A. Strong, in *Proceedings of the Oxford International Conference on Elementary Particles, 1965* (Rutherford High-Energy Laboratory, Harwell, England, 1966); p. A34; D. E. Damouth *et al.*, Phys. Rev. Letters **11**, 287 (1963); C. T. Coffin *et al.*, *ibid.* **15**, 838 (1965); W. Baker *et al.* (unpublished); H. Brody *et al.*, Phys. Rev. Letters **16**, 828 (1966); **16**, 968(E) (1966).

[30] H. H. Atkinson *et al.*, Proc. Roy. Soc. (London) **A289**, 449 (1966).

[31] If the fermion trajectory $\alpha(\sqrt{u})$ contains a linear term in $\sqrt{u}$, then the Regge amplitude by itself can lead to a nonzero polarization. See, for example, J. D. Stack, Phys. Rev. Letters **16**, 286 (1966).

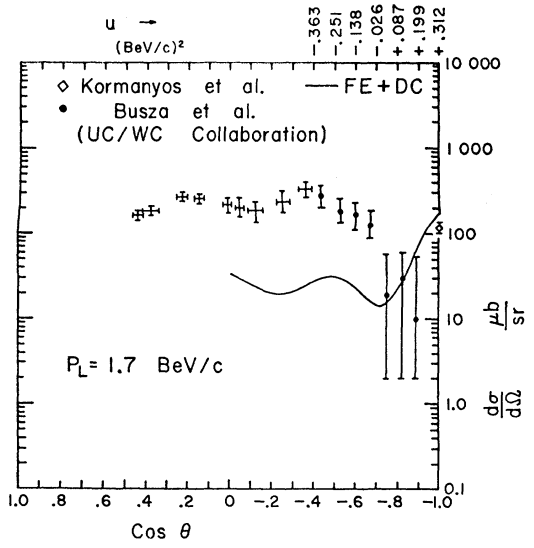
u → (BeV/c)²
−.363 −.251 −.138 −.026 +.087 +.199 +.312
◇ Kormanyos et al. — FE+DC
• Busza et al. (UC/WC Collaboration)
P_L = 1.7 BeV/c
10 000
1 000
100
10
1.0
0.1
dσ/dΩ μb/sr
1.0 .8 .6 .4 .2 0 −.2 −.4 −.6 −.8 −1.0
Cos θ

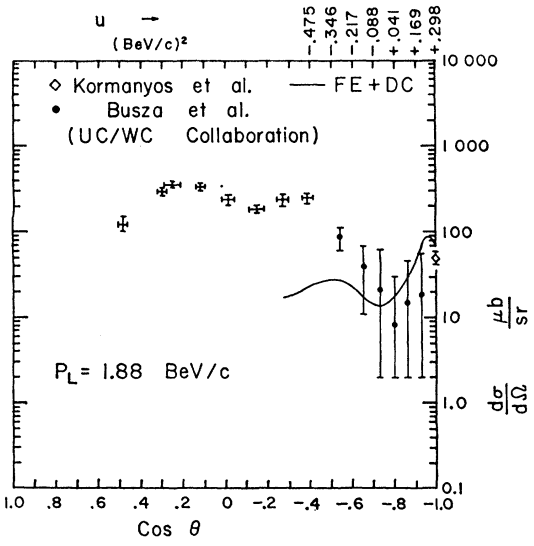
u → (BeV/c)²
−.475 −.346 −.217 −.088 +.041 +.169 +.298
◇ Kormanyos et al. — FE+DC
• Busza et al. (UC/WC Collaboration)
P_L = 1.88 BeV/c
10 000
1 000
100
10
1.0
0.1
dσ/dΩ μb/sr
1.0 .8 .6 .4 .2 0 −.2 −.4 −.6 −.8 −1.0
Cos θ

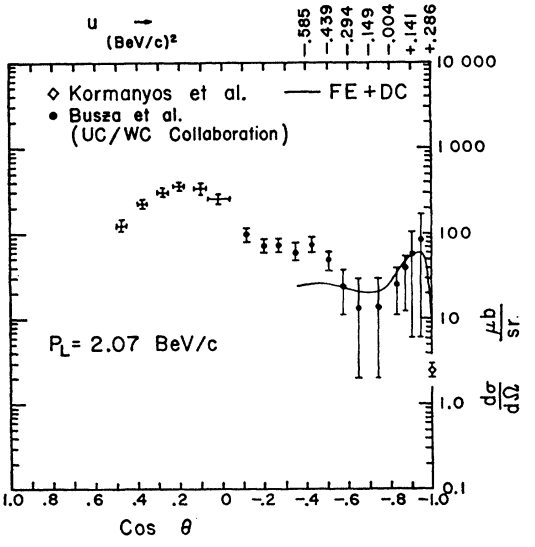
u → (BeV/c)²
−.585 −.439 −.294 −.149 −.004 +.141 +.286
◇ Kormanyos et al. — FE+DC
• Busza et al. (UC/WC Collaboration)
P_L = 2.07 BeV/c
10 000
1 000
100
10
1.0
0.1
dσ/dΩ μb/sr
1.0 .8 .6 .4 .2 0 −.2 −.4 −.6 −.8 −1.0
Cos θ

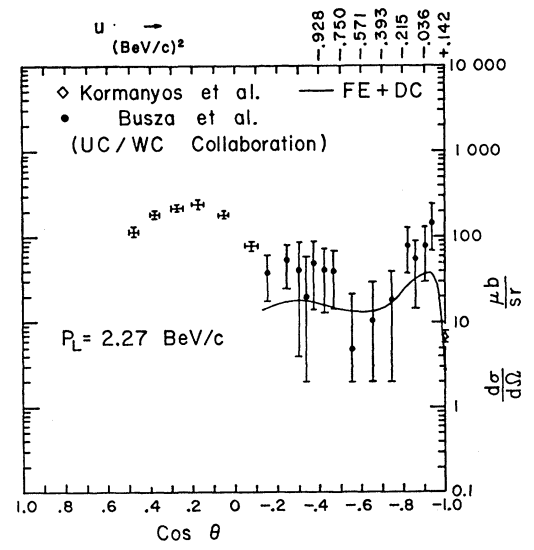
u → (BeV/c)²
−.928 −.750 −.571 −.393 −.215 −.036 +.142
◇ Kormanyos et al. — FE+DC
• Busza et al. (UC/WC Collaboration)
P_L = 2.27 BeV/c
10 000
1 000
100
10
1
0.1
dσ/dΩ μb/sr
1.0 .8 .6 .4 .2 0 −.2 −.4 −.6 −.8 −1.0
Cos θ

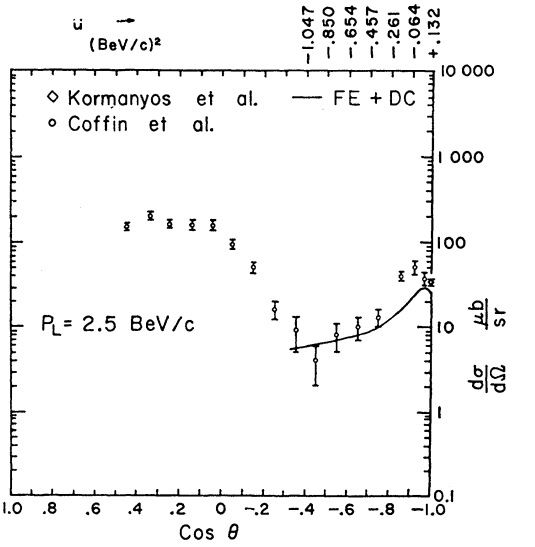
u → (BeV/c)²
−1.047 −.850 −.654 −.457 −.261 −.064 +.132
◇ Kormanyos et al. — FE+DC
○ Coffin et al.
P_L = 2.5 BeV/c
10 000
1 000
100
10
1
0.1
dσ/dΩ μb/sr
1.0 .8 .6 .4 .2 0 −.2 −.4 −.6 −.8 −1.0
Cos θ

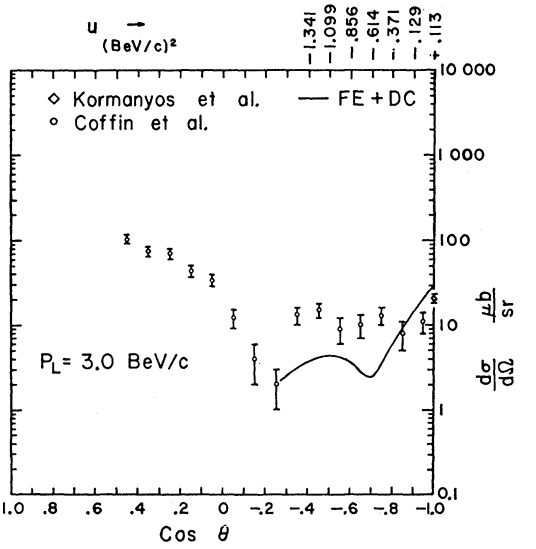
u → (BeV/c)²
−1.341 −1.099 −.856 −.614 −.371 −.129 +.113
◇ Kormanyos et al. — FE+DC
○ Coffin et al.
P_L = 3.0 BeV/c
10 000
1 000
100
10
1
0.1
dσ/dΩ μb/sr
1.0 .8 .6 .4 .2 0 −.2 −.4 −.6 −.8 −1.0
Cos θ

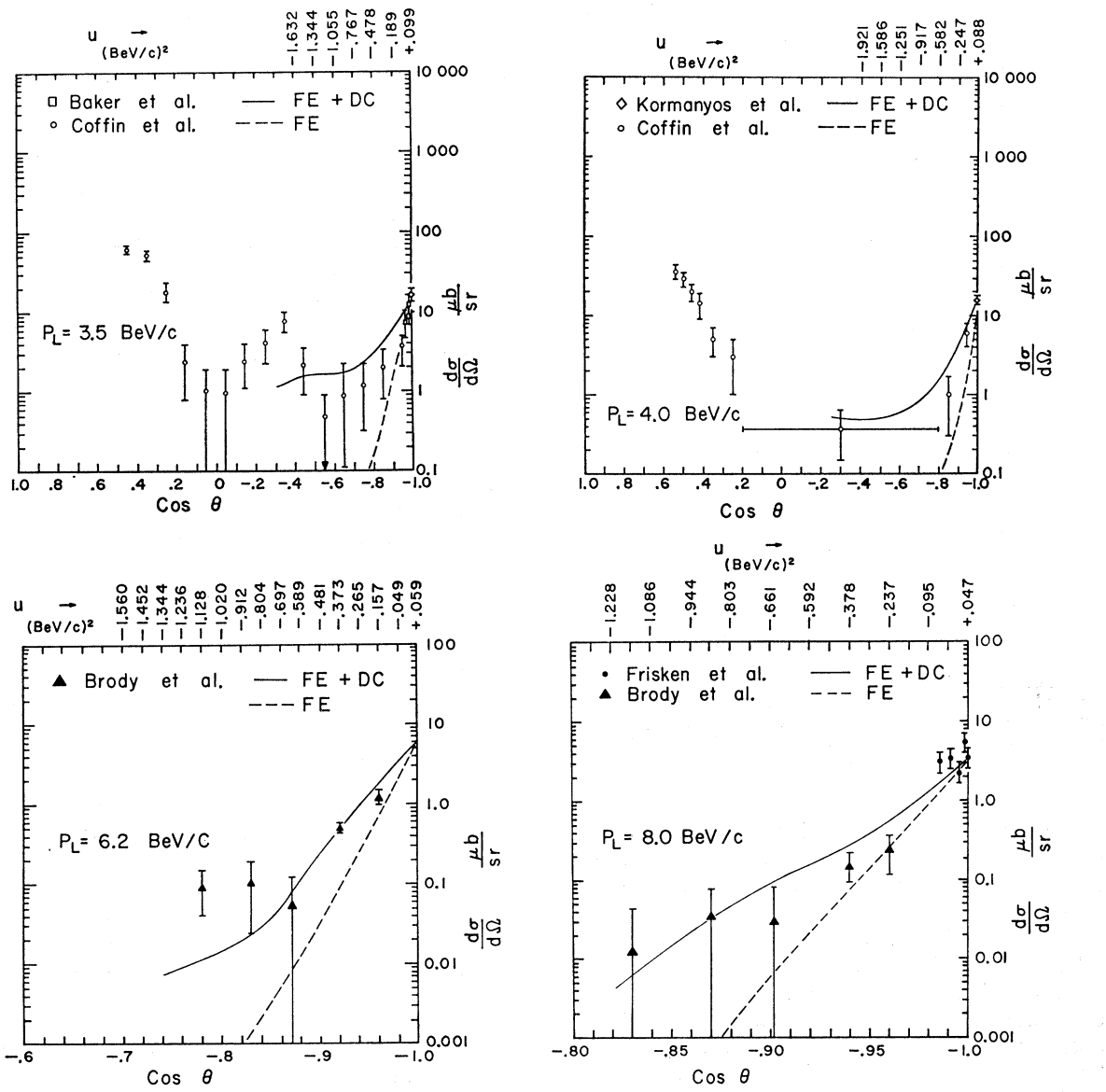

FIG. 5. Theoretical curves for the angular distributions in $\pi^- p$ elastic scattering in the backward hemisphere. The solid curves are based on Δ_δ fermion Regge exchange (FE) plus the direct-channel Δ_δ, N_α, N_γ resonances (DC). The dashed curves represent the contribution of the exchange amplitude alone (FE) to the differential cross sections. The comparison with experiment is made at ten laboratory momenta ranging from 1.7 to 8.0 BeV/c. Experimental data are taken from Refs. 23, 27, and 29.

D. $\pi^+ p$ Elastic Scattering Near 180°

Additional confirmation for the Δ_δ Regge-recurrence parity assignments can be obtained from an analysis of backward $\pi^+ p$ elastic scattering. In the $\pi^+ p$ process, only $I=\frac{3}{2}$ resonances contribute to the direct-channel amplitude, whereas $(\Delta_\delta, N_\alpha, N_\gamma)$ are all allowed as Regge exchanges. With the single exception of a suggested S_{31} resonance at 1690 MeV (see Table I), all the known $I=\frac{3}{2}$ resonances can be assigned to the Δ_δ trajectory, as shown in the Chew-Frautschi plot in Fig. 2(a). In this recurrence classification scheme, all the Δ_δ resonances have the same parity, and thus contribute with the same sign to the direct-channel $\pi^+ p$ backward amplitude [see Eq. (5)]. Also, an additional factor of 3 for the $\pi^+ p$ direct-channel amplitude over the $\pi^- p$ amplitude is acquired from the Δ_δ isotopic-spin Clebsch-Gordan coefficient. The net result of this circumstance is a large direct-channel contribution that appears to saturate the backward $\pi^+ p$ elastic-scattering differential cross section below 4 BeV/c. Significant contributions from the possible Δ_δ, N_α, or N_γ Regge exchanges do not seem to be required to explain the gross features of the $\pi^+ p$ backward elastic-scattering data in the momentum range 0.4 to 4 BeV/c. This situation is markedly differ-

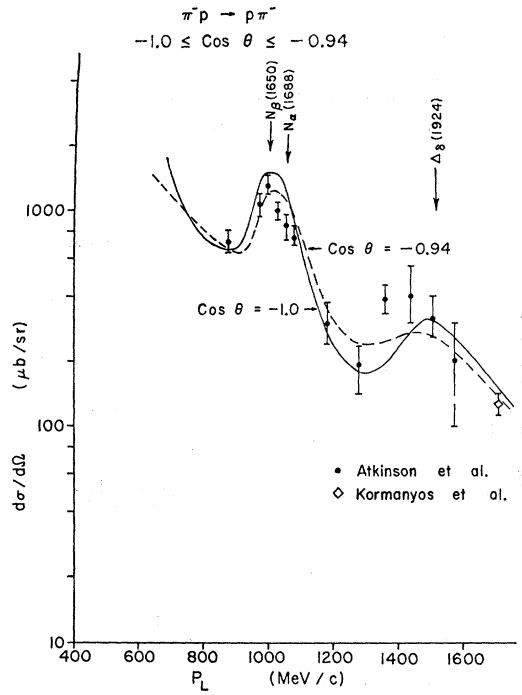

FIG. 6. Comparison of the prediction of the interference model for the backward $\pi^- p$ differential cross sections with the available experimental data at low momenta (600–1900 MeV/c). Experimental data are taken from Refs. 23 and 30. The data points fall in the angular range $-1.0 \leq \cos\theta \leq -0.94$.

ent from the $\pi^- p$ reaction, where appreciable cancellations occurred between the overlapping Δ_δ and N_γ resonances resulting in a direct-channel contribution [see Fig. 3(a)] that was inadequate to explain the 180° $\pi^- p$ experimental data above 2 BeV/c.

The contributions of the Δ_δ resonances to the backward $\pi^+ p$ differential cross section can be immediately calculated from the resonance parameters of Table I obtained from the analysis of backward $\pi^- p$ scattering. The results of such a calculation are compared with the available data[32] in Fig. 8(a) in the momentum range 1.5 to 8 BeV/c. Since only a meager amount of data exists for backward $\pi^+ p$ elastic scattering, it is not possible to compare the model and experimental data at $\cos\theta = -1$, as in the $\pi^- p$ case; instead, the comparison can be made in the angular region of $\cos\theta = -0.94$ to $\cos\theta = -1$. The Δ_δ resonance contribution is in reasonable accord with the experimental near-backward differential cross section up to 4 BeV/c. Additional Δ_δ resonances of higher mass may well account for the discrepancy above 4 BeV/c [conjectured Δ_δ resonances of high mass are indicated in Fig. 2(a)]. Alternatively, an exchange amplitude may play some role in the description of $\pi^+ p$ backward elastic scattering.[19] Inclusion of the Δ_δ-exchange contribution in the $\pi^+ p$ amplitude, with magnitude as determined from the 180° $\pi^- p$ analysis, produces no appreciable perturbation on the Δ_δ direct-channel contribution. Nevertheless, the N_α and N_γ trajectories may also contribute to the exchange amplitude. However, to make an appreciable contribution to $d\sigma/d\Omega$, the residue of an N trajectory would have to be relatively much larger than the Δ_δ residue. The comparative size of the $\pi^- p$ and $\pi^+ p$ differential cross sections is not an indication of the relative magnitude of the Δ and N residues, inasmuch as resonance effects mask the exchange contributions.

In order to test the Regge-recurrence parity assignments of the Δ_δ resonances for this model of backward $\pi^+ p$ elastic scattering, the calculation of the direct-channel amplitude has been repeated with opposite parity assignments for *individual* higher-mass resonances. The results are shown in Fig. 8(b), with $P = -$ for $\Delta(2450)$, and in Fig. 8(c), with $P = -$ for $\Delta(2850)$. Reversal of the parity of either the $\Delta(2450)$ or the $\Delta(2850)$ from its recurrence assignment produces destructive interference with the other direct-channel Δ resonances, and destroys the agreement with the experimental data. Thus, this direct-channel resonance model for $\pi^+ p$ scattering near 180° provides independent confirmation for the suggested Regge-recurrence parity assignments for the $I = \frac{3}{2}$ resonances.[33]

Next, the model was extended to the low-momentum range 400 MeV/c to 1.5 BeV/c. In this range, good agreement with the data could be achieved only by an increase in the elasticity of the $\Delta_\delta(1924)$ resonance (i.e., with $x = 0.5$, as compared with $x = 0.35$ in the $\pi^- p$ analysis)[34] and inclusion of the $\Delta_\beta(1690)$ resonance, which has been suggested by recent phase-shift analyses.[24] This calculation is compared with the experimental data[32] in Fig. 9. Since this model is in qualitative agreement with the data, it supports the existence of the S_{31} resonance at 1690 MeV.

The predicted angular distributions are compared with the limited amount of experimental data[32] below 4 BeV/c in Fig. 10. Again, the agreement is reasonable, except at 3 BeV/c. It is quite possible that a fit to the data, in which resonance parameters are allowed to vary, would produce better agreement. More data will be required before definite conclusions can be reached about the origin of the discrepancy. The predicted angular distributions show considerable shrinkage as a function of laboratory momentum, due to the fact that the recurrence spin assignments increase with the mass

[32] A. I. Alikhanov *et al.*, Phys. Letters **19**, 345 (1965); A. S. Vovenkov *et al.*, JETP Pis'ma v Redaktsiya **2**, 409 (1965) [English transl.: JETP Letters **2**, 255 (1965)]; P. M. Ogden *et al.*, Phys. Rev. **137**, B1115 (1965); H. H. Atkinson *et al.*, Proc. Roy. Soc. (London) **A289**, 449 (1966); J. A. Helland *et al.*, Phys. Rev. **134**, B1062 (1964); F. E. James *et al.*, Phys. Letters **19**, 72 (1965); W. F. Frisken *et al.*, Phys. Rev. Letters **15**, 313 (1965); C. T. Coffin, *ibid.* **17**, 458 (1966); T. Dobrowolski *et al.*, in Proceedings of the Thirteenth International Conference on High-Energy Physics, Berkeley, 1966 (unpublished). For a report of work done by W. Baker *et al.*, see C. T. Coffin *et al.* (Ref. 29).

[33] V. Barger and D. Cline, Phys. Letters **22**, 666 (1966).

[34] At present, it is not known what the precise value of the elasticity of the $\Delta_\delta(1924)$ is. As noted in Table I, any value of x between 0.35 and 0.5 is allowed.

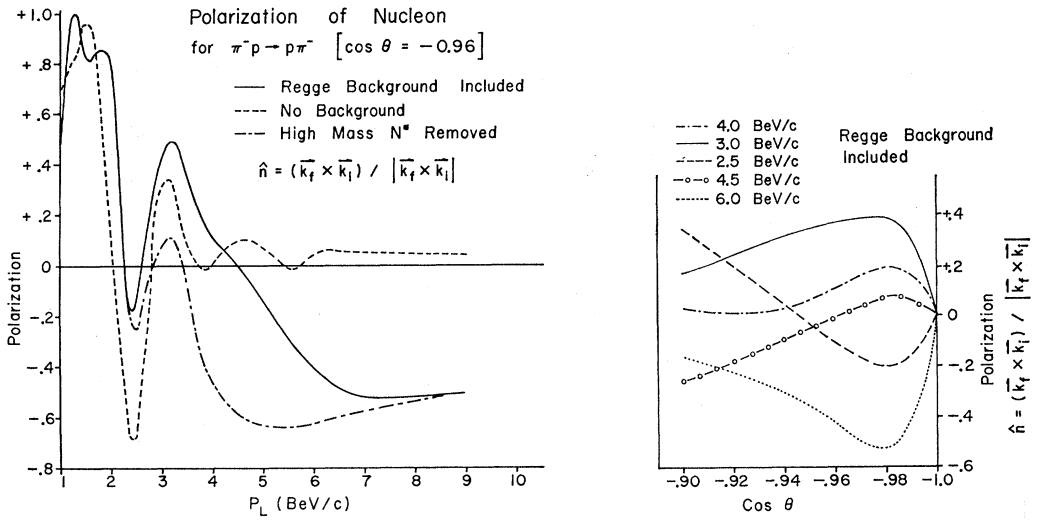

FIG. 7. (a) Prediction for the polarization of the recoil nucleon in $\pi^- p$ elastic scattering as a function of laboratory momentum at the fixed angle of $\cos\theta = -0.96$. The polarization is relative to the unit vector $\hat{n} = (\mathbf{k}_f \times \mathbf{k}_i)/|\mathbf{k}_f \times \mathbf{k}_i|$. The solid curve is based on Δ_δ Regge exchange plus the direct-channel Δ_δ, N_α, N_γ resonances. The dashed curve represents the polarization from the direct-channel resonance amplitude alone. The dash-dot curve indicates the amount of polarization which results from Δ_δ Regge exchange plus only lower-mass direct-channel resonances [i.e., with the $\Delta_\delta(2840)$, $\Delta_\delta(3220)$, $N_\gamma(3020)$, $N_\gamma(3350)$ resonances removed from the direct-channel amplitude]. (b) Angular dependence of the predicted $\pi^- p$ ploarization from the interference model with Δ_δ-exchange and direct-channel resonances.

of the resonances (the Legendre functions of higher l fall off more rapidly with angle near $\cos\theta = -1$). The qualitative success of this model in explaining the present backward $\pi^+ p$ elastic-scattering data suggests that accurate experimental angular distributions might be extremely useful in proving tue Regge-recurrence spin assignments for the Δ_δ resonances. Finally, a further test of the model is provided by the polarization prediction, which is shown in Fig. 11(a), as a function of momentum. The momentum dependence of the polarization is a sensitive measure of the presence of fermion exchange in the u channel. For example, although the Δ_δ exchange produced negligible effects in $d\sigma/d\Omega$ for $\pi^+ p$ scattering, it causes significant structure in the polarization prediction, as shown in Fig. 11(b), Polarization studies will undoubtedly prove to be a very fruitful means of exploring the validity of various models for pion-nucleon backward scattering.

V. DISCUSSION

The twofold intent of this paper was the presentation of plausible Regge-recurrence classifications of the known πN resonances and the construction of a theoretical model for backward πN elastic scattering compatible with these recurrence spin-parity assignments. The comparisons of the model with experiment in Sec. IV are rather favorable and lend considerable support to the validity of the parity assignments for the resonances and some support to the Regge theory for the fermion-exchange amplitude. Further tests of the model can be made as soon as polarization measurements and more detailed angular distributions become available.

One of the more interesting aspects emerging from the calculations concerns the nature of the contributions of the resonances to the direct-channel amplitude. The resonance width in the laboratory frame $\Gamma_{\text{lab}} = (M_R/M)\,\Gamma_{\text{c.m.}}$ increases because of the mass factor (M_R/M) and the experimental increase in $\Gamma_{\text{c.m.}}$ (see Table I). Consequently, the contributions of a high-mass resonance extend over a broad range of laboratory momomenta. An illustration of this feature is shown in Fig. 12, where the arrow tips denote the values $\epsilon = \pm 2$ for resonance forms proportional to $1/(\epsilon - i)$. At $|\epsilon| = 2$, the imaginary part $1/(\epsilon^2+1)$ has decreased to $\frac{1}{5}$ of its maximum value, but the tail due to the real part $\epsilon/(\epsilon^2+1)$ continues to make sizeable contributions for $|\epsilon| > 2$. Since the resonance tails are certainly important, at least to $|\epsilon| \simeq 2$, the contributions of the individual resonances to the direct-channel amplitude overlap considerably at any given laboratory momentum, as indicated in Fig. 12. As a result, the situation becomes markedly different from customary considerations for an isolated resonance. The extent to which the Breit-Wigner resonance form remains an adequate approximation at some distance from the resonance position takes on a somewhat greater importance, particularly for the real part of the resonance amplitude which dies off rather slowly. If centrifugal barrier factors[11,35] of the form $(qR)^{2l+1}/D_l(qR)$ [where $D_l(qR) \to (qR)^{2l}$ for very large qR] are incorporated

[35] R. D. Tripp, CERN Report No. 65-7 (Rev.), 1965 (unpublished), p. 11.

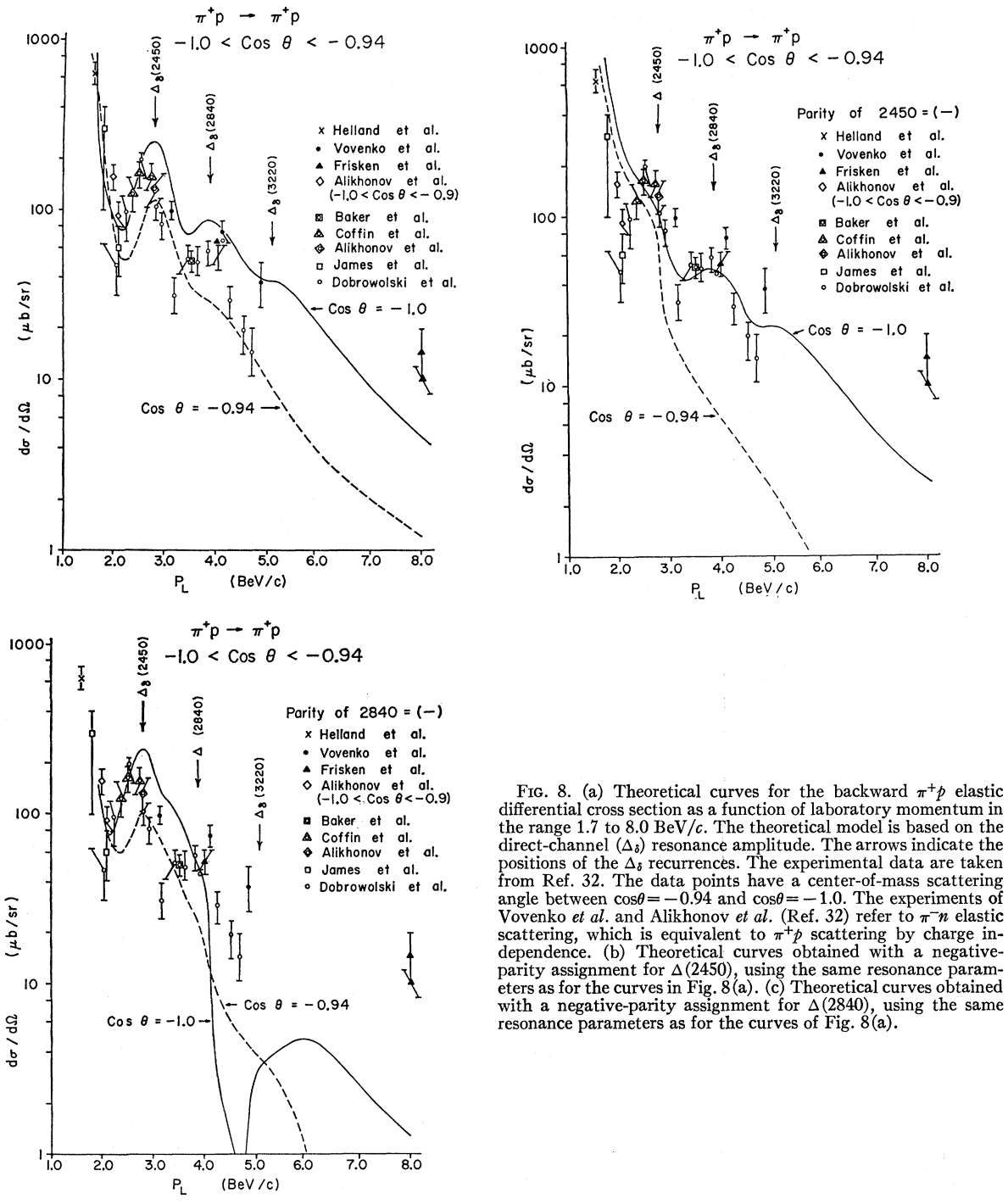

FIG. 8. (a) Theoretical curves for the backward π^+p elastic differential cross section as a function of laboratory momentum in the range 1.7 to 8.0 BeV/c. The theoretical model is based on the direct-channel (Δ_δ) resonance amplitude. The arrows indicate the positions of the Δ_δ recurrences. The experimental data are taken from Ref. 32. The data points have a center-of-mass scattering angle between $\cos\theta = -0.94$ and $\cos\theta = -1.0$. The experiments of Vovenko *et al.* and Alikhonov *et al.* (Ref. 32) refer to π^-n elastic scattering, which is equivalent to π^+p scattering by charge independence. (b) Theoretical curves obtained with a negative-parity assignment for $\Delta(2450)$, using the same resonance parameters as for the curves in Fig. 8(a). (c) Theoretical curves obtained with a negative-parity assignment for $\Delta(2840)$, using the same resonance parameters as for the curves of Fig. 8(a).

into the expressions for the total and elastic widths, then $\Gamma \sim q$ and resonances tend to make even larger contributions far above the resonance position. On the other hand, at energies above the resonance mass, further inelastic channels become kinematically accessible to the resonance, which probably results in the elasticity parameter being driven down as a function of increasing energy. In the present analysis we have not attempted to explore such behavior for the widths in the Breit-Wigner resonance amplitudes in detail, because the resonance parameters from previous analyses were not determined in such a fashion.

The schematic diagram in Fig. 12 reveals that resonance effects are also present at relatively high mo-

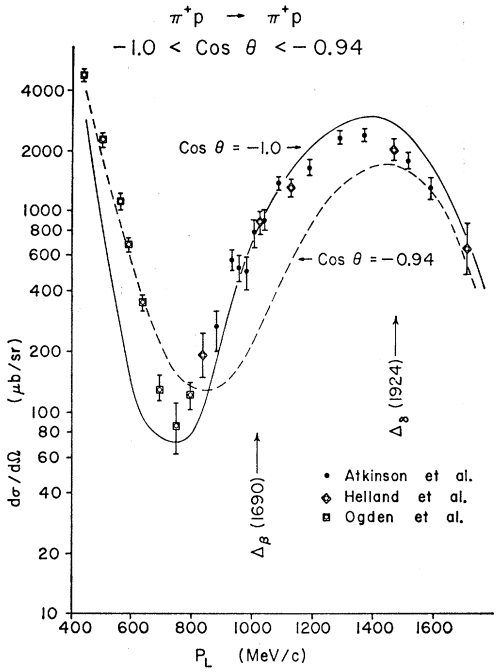

FIG. 9. Theoretical curve for the backward π^+p elastic differential cross section at low momenta (400 to 1600 MeV/c). The calculation is based only on direct-channel Δ resonances. The experimental data are taken from Ref. 32. The data points have a center-of-mass scattering angle between $\cos\theta = -0.94$ and $\cos\theta = -1.0$.

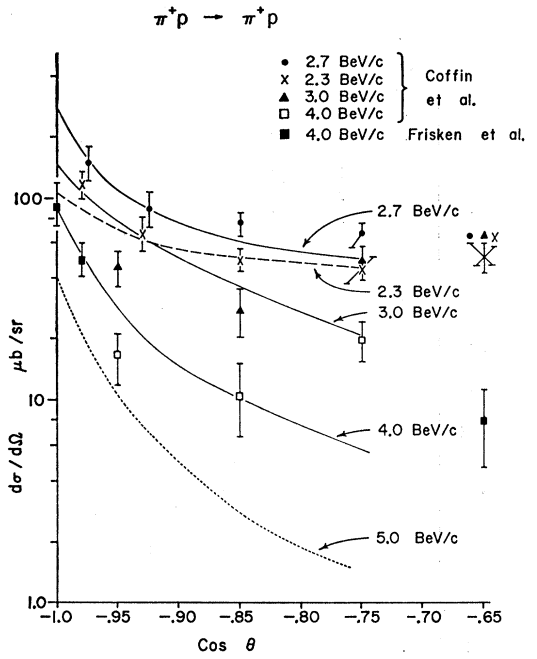

FIG. 10. Predicted angular distribution for backward π^+p elastic scattering from the direct-channel Δ_δ resonance model. The experimental data are taken from Ref. 32.

menta (note that the laboratory-momentum position of a high-mass resonance is $P_{\text{lab}} \simeq M_R^2/2M_N$). The *known* resonances can give non-negligible contributions to the direct-channel amplitude even at 5 BeV/c, a fact that is not normally realized in phenomenological calculations. [The polarization predictions at high momenta are particularly sensitive to the direct-channel resonances (see Sec. IV).] As a further complication, it seems quite conceivable that resonances of even higher mass will eventually be discovered.

It is an interesting empirical fact that the elastic widths decrease rapidly with increasing resonance mass (see Table I). This may be interpreted as due in part to centrifugal barrier suppression, since the angular momenta of the resonances increase quadratically with mass in the Regge-recurrence model. However, a detailed calculation of barrier factors requires knowledge of the radii of interaction. In Fig. 13 the decrease of the

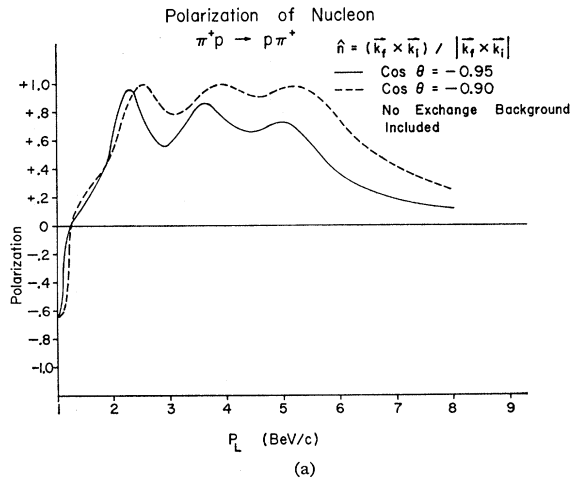

FIG. 11. Theoretical predictions for the polarization of the final nucleon in π^+p elastic scattering near the backward direction. (a) Direct channel Δ_δ resonance model for the laboratory momentum range 1 to 8.0 BeV/c. (b) Direct-channel Δ_δ resonances plus Δ_δ Regge-exchange model for the momentum range 1 to 8.0 BeV/c.

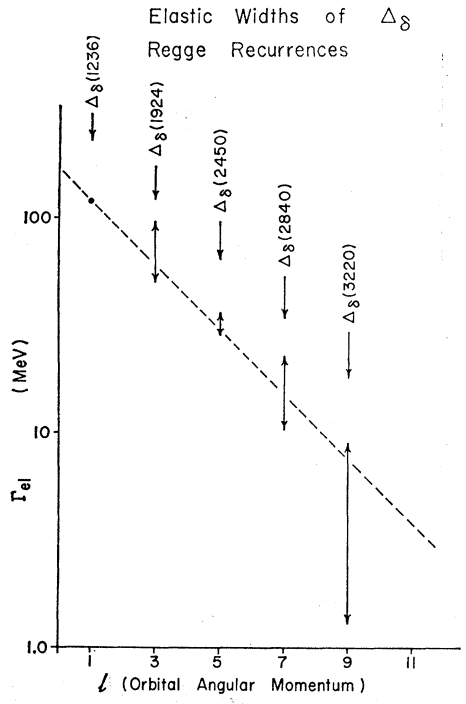

FIG. 12. Illustration of the extent to which the direct-channel resonances overlap and contribute at high momenta. The arrow tips denote the values $\epsilon=\pm 2$ for resonance forms proportional to $1/(\epsilon-i)$.

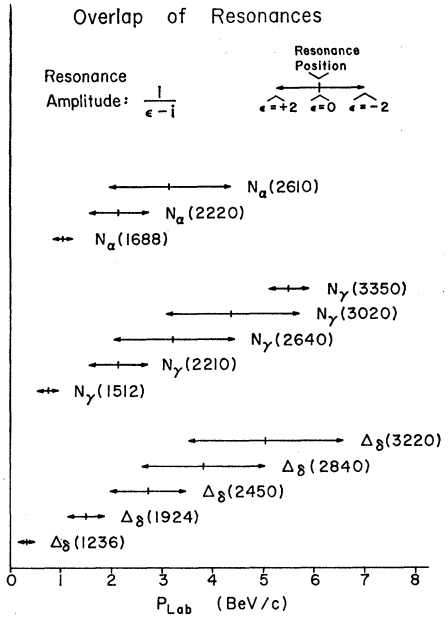

FIG. 13. Elastic widths of the Δ_δ resonance versus orbital angular momentum l. The l values are deduced from the Regge-recurrence J^P assignments. The arrow tips denote reasonable uncertainties in the determinations of the elastic widths.

elastic widths for the Δ_δ resonances is illustrated. The fall-off may be exponential in l (equivalently M^2) or even more rapid. Using this empirical relationship, it should be possible to estimate the elastic widths of the conjectured higher-mass resonances in Fig. 2. If resonances with such elastic widths can be excluded experimentally, this might serve as an indication that trajectories do not indefinitely remain linear.

An interference model of the type proposed here for backward πN scattering has certain limitations. Even if this model is valid at 180°, it is expected to break down as $\cos\theta$ increases from -1.0. In the first place, the tail of the forward diffraction peak extends to

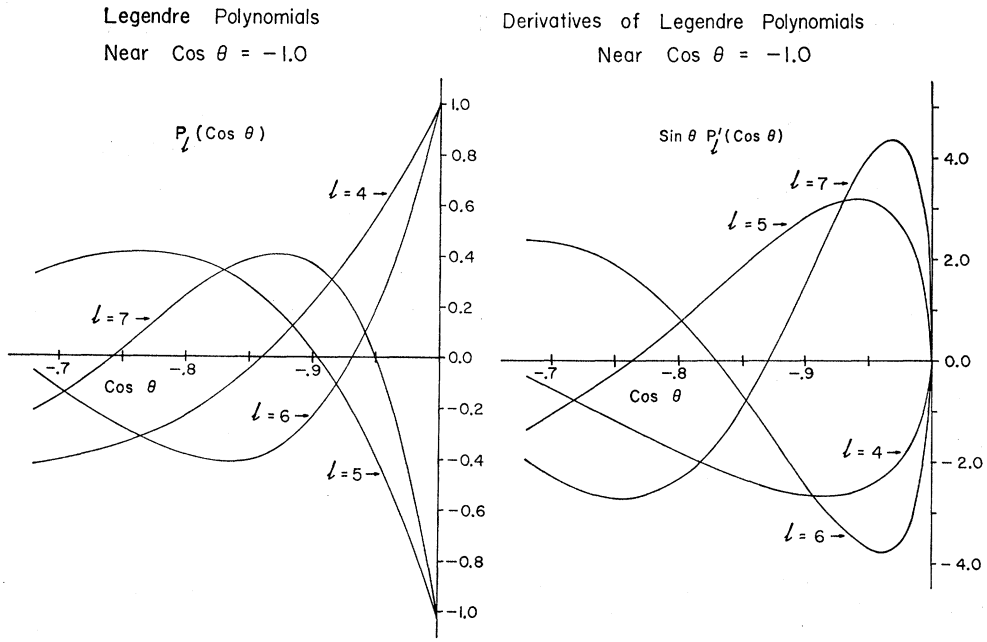

FIG. 14. Illustration of oscillations in Legendre polynomials of high l near $\cos\theta=-1$:
(a) $P_l(\cos\theta)$,
(b) $\sin\theta dP_l(\cos\theta)/d\cos\theta$.

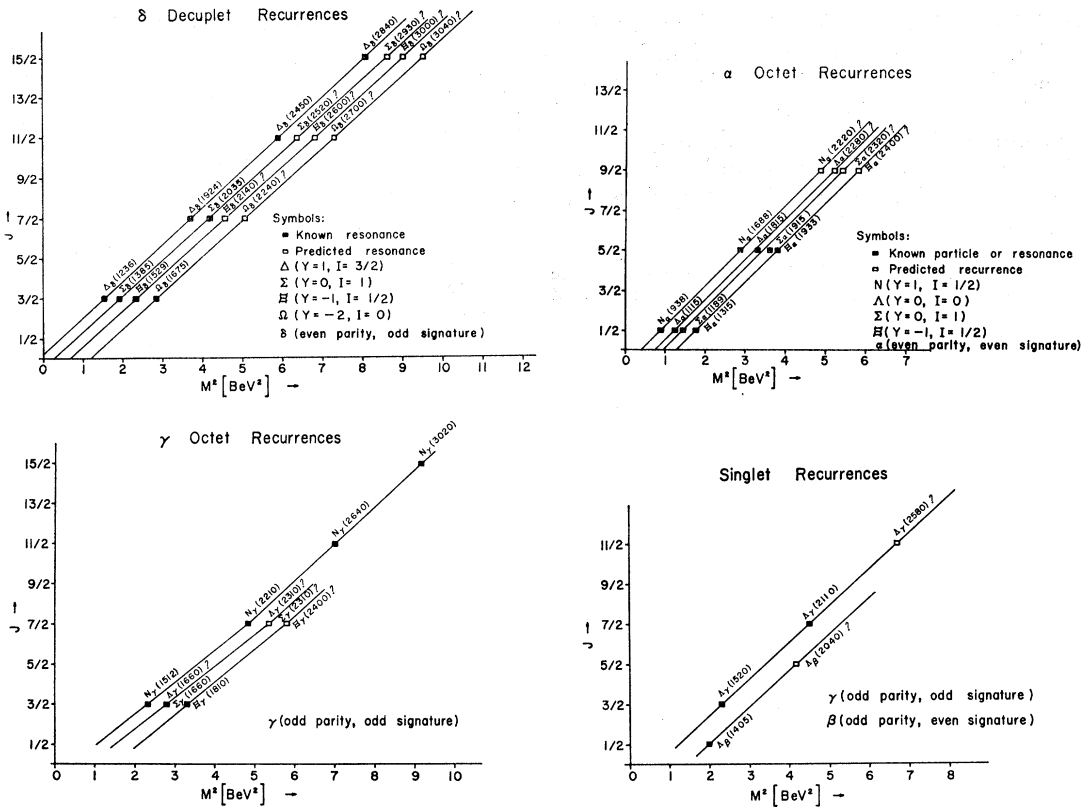

FIG. 15. Chew-Frautschi plots of fermion Regge recurrences classified according to **1**, **8**, and **10** representations of $SU(3)$: (a) δ decuplet recurrences, (b) α octet recurrences, (c) γ octet recurrences, (d) β and γ singlet recurrences.

relatively large angles at low-laboratory momenta [see Figs. 5(a), 5(b), 5(c)]. Secondly, resonances which provide the dominant contribution to the amplitude at $\cos\theta=-1$ will not necessarily continue to dominate at other angles. In particular, since the number of oscillations of Legendre functions increases with l [for illustration see Figs. 14(a) and 14(b)], the model may only be valid in a narrower angular cone as the momentum increases. Thus, if lower spin resonances exist, they would probably be of much greater importance away from $\cos\theta=-1.0$. Deviations of the types suggested above presumably account for the qualitative discrepancies away from $\cos\theta=-1.0$ in Fig. 5.

Recently, the interference model has been applied to (i) the differential cross section of the $\pi^-p\to\pi^0n$ reaction at $t=-0.09$ (BeV/c)^2 (using Regge ρ-meson exchange)[36] and (ii) the polarization in $\pi^\pm p$ elastic scattering near the forward direction (using P, P', ρ-meson exchanges).[37] When compared with the experimental data, the results of these calculations lend additional support to the interference model and to the Regge-recurrence assignments. A convincing argument in support of the interference model is the fact that consistent results are obtained for reactions with exchange amplitudes of quite different phase. For example, with ρ-meson exchange in $\pi^-p\to\pi^0n$ at 0°, the phase is roughly $e^{i\pi/4}$, whereas with Δ_δ exchange in $\pi^-p\to p\pi^-$ at 180°, the phase is roughly $e^{i3\pi/4}$.

We anticipate that the methods developed in this paper will also be useful in the classification of $Y\neq1$ fermion states and the description of processes involving the exchange of these systems. An extended Regge-recurrence classification scheme including the $Y=1$, 0, -1, -2 resonances[2] is shown in Fig. 15, where the fermion states are grouped in terms of singlet, octet, and decuplet representations of $SU(3)$. This classification scheme is attractive, in that it incorporates *only* one-, eight-, and ten-dimensional $SU(3)$ representations with the Regge-recurrence hypothesis, but is obviously not known to be a unique classification.[38] Nevertheless, certain general features of this classification will undoubtedly survive in the ultimate assignments of these resonances. Namely, since the extrapolated intercepts

[36] J. Baacke and M. Yvert, in Proceedings of the Thirteenth International Conference on High-Energy Physics, Berkeley, 1966 (unpublished).

[37] P. D. Grannis, H. M. Steiner, and L. Valentin, in Proceedings of the Thirteenth International Conference on High-Energy Physics, Berkeley, 1966 (unpublished).

[38] In addition to the resonances shown in Fig. 15, there are some known $Y=1$ (see Table I) and $Y=0$ (see Ref. 2) resonances which as yet are not classified in the Regge-recurrence scheme.

at $u=0$ of the $Y\neq 1$ trajectories fall considerably lower than the intercepts of the $Y=1$ trajectories, the backward differential cross sections for reactions dominated by the exchange of the $Y\neq 1$ fermion systems should decrease more rapidly with energy in the Regge model than the corresponding situations with $Y=+1$ exchange. Further detailed investigations along these lines should prove to be of great interest.[39]

[39] We are presently extending the interference model to the reactions $Kp\to pK$, $Kp\to \Xi K$, and $\pi p\to \Sigma K$ for backward scattering.

ACKNOWLEDGMENTS

We have benefited from discussions with numerous physicists at the University of Wisconsin, the University of Michigan, and the Lawrence Radiation Laboratory. One of us (V.B.) would like to thank Professor G. F. Chew for the hospitality of the Lawrence Radiation Laboratory and, in addition, Professor E. M. Henley and Professor B. A. Jacobson for the hospitality of the Summer Institute for Theoretical Physics at the University of Washington.